Category UC-126

SAND88-3262
Unlimited Release
Printing July 1989

RADAR LOGGING OF STORAGE CAVERN WALLS AT THE STRATEGIC PETROLEUM RESERVE: A FEASIBILITY ESTIMATE

J. G. Castle
SPR Geotechnical Division 6257
Sandia National Laboratories
Albuquerque, New Mexico 87185-5800

ABSTRACT

The feasibility of using a radar logging tool to map the salt walls in the caverns storing crude oil at the Strategic Petroleum Reserve (SPR) is examined. The tool design has dimensions small enough to permit entry into every SPR cavern at Big Hill, Bayou Choctaw, West Hackberry, and Bryan Mound, is able to resolve wall features as small as five feet, and can measure the range to the cavern wall with an uncertainty less than one foot. Usable radar echoes are predicted if the walls are very rough in 37 of the 45 storage caverns during operation at 1 GHz. Dependence on frequency and wall roughness is presented. Very strong echoes are to be expected in most caverns at 1 GHz.

TABLE OF CONTENTS

		Page
1	INTRODUCTION	1
1.1	SPR Cavern Shapes: What Is Known	1
1.2	Cavern Wall Contours: Mapping Needs	2
1.3	Tool Constraints and Development Options	3
1.4	Purpose and Scope	4
1.5	Approach Taken	4
2	RADAR ANTENNA CHOSEN AND ITS RADIATION PATTERN	6
2.1	A Useful Horn Design	7
2.2	Vertical Array of Horns	7
2.3	Resolution at Cavern Wall	8
2.4	Available Loop Sensitivity (ALS)	9
3	ECHO ATTENUATION	9
3.1	Dielectric Constant and Loss Tangent in SPR Crudes	9
3.2	Correlation of Loss Tangent with Sulphur Content	10
3.3	Echo Attentuation in SPR Caverns	10
4	CAVERN WALL CONDITION	10
4.1	Salt-Oil Reflection Coefficient	11
4.2	Wall Roughness and Contour	11
5	RADAR S/N CALCULATED FOR SPR CAVERNS	11
6	CONCLUSIONS	14
7	RECOMMENDATIONS	15
8	ACKNOWLEDGEMENTS	16
9	REFERENCES	16
	GLOSSARY	17

APPENDIX A. CALCULATION OF RADAR ECHOES IN SPR CAVERNS

APPENDIX B. SPREADSHEET LISTING OF RADAR S/N FOR SPR CAVERNS

TABLE OF CONTENTS OF APPENDIX A

		Page
Al	SCOPE OF APPENDIX A	Al
A2	ACCURACY EXPECTED IN RADAR RANGE VALUES	Al
A2.1	Range Spread from Wall Roughness	A2
A2.2	Time of Arrival of Echo	A2
A2.3	Dielectric Constants of SPR Oils	A3
A3	RADIATION PATTERN OF ANTENNA ARRAY	A3
A4	THE RADAR EQUATION FOR CAVERN MAPPING	A6
A4.1	Modifying the Radar Equation for Wall Mapping	A6
A4.1.1	Directivity of Antenna	A7
A4.1.2	Truncate Pattern of Incident Power Flux	A8
A4.1.3	Power Reradiated from Wall	A8
A4.1.4	The Modified Radar Equation	A9
A4.2	Radar Equation for Matte Finish Wall Condition	A9
A4.3	Radar Equation for Very Rough Wall Condition	A10
A5	ATTENUATION IN SPR CRUDE OILS	All
A5.1	Loss Tangents Observed for Six SPR Caverns	All
A5.2	An Expression for Tan6 versus SULPHUR	Al2
A5.3	Power Transmission of Cavern Oil	Al3
A6	AVAILABLE LOOP SENSITIVITY FOR RADAR TOOL	A13
A7	EXPECTED SIGNAL-TO-NOISE (S/N)	A15

TABLE OF FIGURES

Page

2.3 Vertical section of cavern containing radar array..... 8
5.1 Radar S/N expected at 1 GHz in SPR caverns with a very rough wall patch at CReff..... 12
5.2 Radar S/N expected at 1 GHz in SPR caverns with a matte finish wall patch at CReff..... 12
5.3 Radar S/N expected at 1 GHz in SPR caverns with a very rough wall patch at CRmin..... 13
5.4 Radar S/N expected at 1 GHz in SPR caverns with a matte finish wall patch at CRmin..... 13

APPENDIX A:

A3 Antenna radiation pattern for 1 GHz in SPR oil..... A5
A5.2 Fit of expression for tan6 to observed tanδ..... Al2
A7.1 Radar S/N expected at 1.4 GHz in SPR caverns with a very rough wall patch at CReff..... A16
A7.2 Radar S/N expected at 1.4 GHz in SPR caverns with a matte wall patch at CReff..... A16
A7.3 Radar S/N expected at 1.4 GHz in SPR caverns with a very rough wall patch at CRmin..... Al7
A7.4 Radar S/N expected at 1.4 GHz in SPR caverns with a matte wall patch at CRmin..... Al7
A7.5 Radar S/N expected at 2 GHz in SPR caverns with a very rough wall patch at CReff..... Al8
A7.6 Radar S/N expected at 2 GHz in SPR caverns with a matte wall patch at CReff..... Al8
A7.7 Radar S/N expected at 2 GHz in SPR caverns with a very rough wall Patch at CRmin..... Al9
A7.8 Radar S/N expected at 2 GHz in SPR caverns with a matte wall patch at CRmin..... Al9

TABLE OF TABLES

Page

5 Summary of radar S/N predicted for 45 SPR caverns..... 14

APPENDIX A:

A3 Calculated features of radiation patterns..... A4
A5.1 Microwave loss tangents, dielectric constants, and sulphur concentrations observed in SPR crude oils..... All

APPENDIX B:

Spreadsheet calculation of S/N for SPR caverns..... B2

1 INTRODUCTION

1.1 SPR Cavern Shapes: What Is Known

The U. S. Strategic Petroleum Reserve (SPR) stores crude oil in man-made caverns that have been leached into large salt domes near the coast of Louisiana and Texas. During SPR Phase I in the late 1970's and early 1980's, crude oil was stored in caverns that had been previously leached for commercial brine production. To assure stability and to control the effect of salt creep, a standard cavern design in the shape of a tall right-circular cylinder with a dome roof was developed. Most of the current inventory of 565 million barrels of crude is stored in caverns whose shape closely resembles the standard design. Preservation of the crude oil inventory by continued assurance of cavern integrity has a high priority in the operation of SPR.[1-3]

A standard SPR storage cavern holds ten million barrels of crude oil and initially one million barrels of brine. The standard cavern has a height of 2000 feet, an effective cavern radius of 100 feet, and a slight decrease in the radius from top to bottom. The salt cavern will creep steadily inward due to the external pressure being greater than pressure from the stored oil. This creep will reduce cavern volume by some ten percent over 30 years of quiescent storage.

The walls of some of the storage caverns are known to have irregularities. The only source of information on the actual contours of SPR caverns are sonar surveys done through brine before crude oil injection. Some Phase I caverns have ledges, overhangs, washouts, etc. The long-term integrity of these caverns is less certain than for the quasi-cylindrical ones.

Some of the cylindrical caverns are also known to have irregular wall features. These features include roof irregularities and radial elongations. The latter tend to be associated with preferential leaching of the salt. In addition, evidence of occasional salt falls appears as damage to hanging strings and the associated buildup of salt on the cavern floor.

There is currently no logging tool available in this country capable of assessing the origin of such salt falls or monitoring wall stability in caverns as large as 100 feet in radius in oil-filled caverns.' The sonar and radar options for possible tool development to serve this function are mentioned in Sec. 1.3. The Prakla-Seismos sonar tool, available in West German, has routinely mapped the walls of much smaller (2MMBL) crude oil caverns.5 The tool has also demonstrated the capability to receive sonar

returns at 180 feet in very light North Sea oils. The tool has never been tested in more viscous oils characteristic of SPR due to the high cost of demonstrating the tool in this country. Mapping of irregular wall features with sufficient resolution to confirm that their shapes are remaining stable would provide significant assurance. Such maps would also provide a method of inventorying stored oil.

The economic incentive for development of an oil-filled cavern mapping tool is high. Currently, in order to assess or monitor cavern changes, oil must be displaced by brine to permit sonar mapping. The cost of removing oil (drawdown) from a single cavern is in the range of $2.5 million dollars. This doesn't include the cost of alternate storage or reduction in life of the cavern. Eliminating the need for drawdown of a single cavern would more than offset expected tool cost.

1.2 Cavern Wall Contours: happing Needs

During the development of a SPR cavern, it is usually mapped with sonar in sections after each section is leached to ~200-foot diameter. Each survey is run in brine prior to oil displacement of the brine in that section. Consider the precision presently available from these sonar surveys.

A sonar logging tool, operated at 250 kHz, is deployed near the centerline of the cavern for mapping. Spatial resolution is approximately a lo-foot diameter circle at the wall. The sonar transducer (antenna) at the lower end of the logging tool rotates the full 360-degree azimuth at each of a series of depths, usually every 20 feet. Sonar echoes are received from different features of an irregular wall surface when the features are contained within the lo-foot circle. The usual data processing produces only a single value for the time of arrival. We presume this is the time of first arrival of an echo above some selected power level. Values of the time of arrival are converted to range at 128 equally spaced directions per revolution.

The resulting sonar maps show an abrupt change in range at many of the detected irregularities in the wall. These abrupt changes in range are often larger than 10 feet. Some of this uncertainty may arise from variations in wall roughness as well as changes on radius. Range accuracy specifications of ± 5 percent are typical, with angular resolutions of about .03 radians made possible by operation at 250 kHz.

Following oil fill, such tools have to be operated at much lower frequencies, typical less than 40 kHz due to the high attenuation of sonar at higher frequencies. (The attenuation is nearly proportional to

frequency.) At the lower frequencies, although sonic returns occur, the angular resolution of the sonar system is extremely poor (two radians), making usefulness of the data very low.

Specific resolution requirements in the surveys of oil-filled SPR caverns have not yet been established. A sonar or radar tool which resolved wall features as close together as five feet and resolved changes in range smaller than one foot would offer the following advantages:

a. Monitoring the stability of irregular wall features as small as five feet across to within one foot in radial position.
b. Inventory of stored oil to a precision of better than 5%.
c. Provide an independent measurement of the calculated creep of the cavern wall, which has been predicted to approach one foot per year in the lower third of the cavern.

1.3 Tool Constraints and Development Options

Oil-filled SPR caverns have been surveyed with sonar with limited success.' The oil attenuates the 250 kHz energy too severely at the range of 100 feet. A survey at lower frequency yielded detectable echoes but angular resolution of several radians. There is a potential of usable echoes from a multiple-frequency tool that has been used in smaller oil-filled caverns in West Germany.5

The only way to obtain improved angular resolution from a sonar or radar tool located near the cavern centerline is to increase the directivity or gain of the antenna. This is accomplished by an increase in the number of wavelengths that fit across the aperture of the antenna (transducer). An aperture width of 20 wavelengths will resolve wall features closer together than 5 feet in azimuth provided the oil is sufficiently uniform along the path of the echoes. Similarly, an antenna (transducer) height of 20 wavelengths in oil will resolve wall features closer together in height than 5 feet.

There are two ways to increase the number of wavelengths that fit within the aperture. One is to increase the frequency of the waves in the oil. The other is to increase the effective size of the aperture of the antenna (transducer) array. The constraint on the upper frequency limit is set by the attenuation within the oil.6 The maximum tool diameter for access to SPR caverns through the 13 5/8-inch OD pipe casing is one foot OD. Insertion through the required lubricator limits the tool length to approximately 25 feet. The compromise on the size of the aperture is set by the complexity of supporting and driving a large array, which folds to pass through the wellhead casing. An acceptable logging rate is thought to

be based on a complete scan of the cavern wall in 24 hours plus the time for insertion and extraction of the tool. The design used for this feasibility calculation meets these constraints.

Resolution of wall features five feet apart requires, as mentioned above, the effective antenna aperture dimensions to be 20 wavelengths. For sonar at 40 kHz, the phase-controlled transducer array would cover more than two feet. For radar at 14 GHz, the aperture would be only 0.9 feet, but the attenuation is known to be too severe for the 100-foot range required for SPR caverns." For radar at 1 GHz, the phase-controlled array would cover some 13 feet.

1.4 Purpose and Scope

The purpose of this report is to estimate the detectability of return signals in terms of the system signal-to-noise ratio (S/N) of a radar tool which operates near 1 GHz, resolves wall features less than five feet across, and records the range to the wall with an accuracy of one foot. The basis of attenuation calculations in each of the 45 caverns is recent data taken on oil samples from six of the SPR caverns.6 The present report establishes one combination of radar system characteristics which could serve as a useful logging tool at SPR.

The scope of this report is limited to the calculation of radar signal returns anticipated from "rough" and "smooth" walls in each storage cavern at the SPR sites of Bryan Mound, West Hackberry, and Bayou Choctaw.7 The results highlight the tradeoffs between frequencies near 1 GHz for a fixed antenna size.

1.5 Approach Taken

This analysis of S/N is based on assumptions summarized here and discussed in detail in Appendix A. The assumptions are conservative, aiming for realistic values of S/N. The approach is to start with the radar equation[8-11] valid for distant targets that are much smaller than the antenna beam width, and to adapt the radar equation as needed for each specific wall condition.

The frequency of the waves generated in the oil by the mapping tool is a crucial parameter. For a given antenna size, the resolution at the wall improves in direct proportion to the frequency. However, wave attenuation in the oil during the trip to the wall and back is nearly proportional to the frequency. The necessary compromise is investigated in this study by considering only the three frequencies, 1.0, 1.43, and 2.0 GHz.

Resolution of wall features that are separated vertically by less than five feet at 100 feet cavern radius fits the SPR need as noted above. For this study, we choose fixed antenna dimensions and equate this resolution value to the distance between the locations at which the incident intensity is down to one-half the maximum intensity. These 3-dB locations are separated by the angle in the antenna radiation pattern called the half-power beam width (HPBW). That angle in elevation, HPBWev, is 0.044 radians or 4.4 feet at 100 feet when the antenna array has a vertical span of 20 wavelengths. The wavelength is ~2/3 foot in SPR crudes[6] at 1 GHz. So we choose the height of the antenna array to be 13.3 feet. At 2 GHz, the same size array spans 40 wavelengths and its radiation pattern would resolve 2.2 feet at 100 feet.

Horizontal resolution of wall features is controlled by the horizontal width of the array. The best resolution comes with the largest width, which we limit to -90 percent of the tool diameter for mechanical strength. The resulting half-power beam width in azimuth, HPBWaz, is rather large. It would probably be worthwhile for such a tool to be capable of tilting the array up to -90 degrees. Such a capability would allow the excellent resolution arising from the 4-meter length to be used horizontally to scan the elongations of radius that exist as tall features in some cavern walls.

Determination of distance to the wall with an uncertainty of less than one foot is feasible when the return signals are strong provided the signal bandwidth is at least 50 MHz. Adding together the time profile of eight successive returns would give an effective noise bandwidth (B,) of 20 MHz. In this report, B_n is assumed to be 50 MHz.

The loss tangent of the oil in each cavern is calculated by assuming that the tentative correlation we have recently found between total sulphur concentration and tan6 in six crudes applies to all the SPR crudes. Most of the estimated uncertainty of ± -10 dB in echo strength is due to lack of knowledge of the actual loss tangent values for the oil stored in each cavern. Water is assumed to have dropped out of SPR crude oil that has been stored for several years; hence, the variations in dielectric properties arise primarily from the polar hydrocarbons, such as the mercaptans that are known to be present.8

Effects of wall roughness are ilustrated by comparing two extreme conditions. For a very rough wall, i.e., rough on the scale of several wavelengths, we assume that the wall scatters isotropically and incoherently. For a smooth wall, i.e., smooth on the scale of one wavelength and rough on a small scale much less than 1/4 wavelength, reflection or reradiation is assumed to be isotropic and coherent. This roughness only on small scale is labelled a matte finish. We assume

throughout this preliminary estimate, that the wall is a right circular cylinder with the tool on the cavern's centerline. Operation off the centerline is affected by unequal attenuation over unequal ranges and by reduced return due to the reradiation pattern of a non-cylindrical wall. Both of these effects will be small in most SPR caverns.

It should be noted that a smooth portion of wall that is curved to reflect the return beam away from the centerline could drop the direct return signal by several orders of magnitude. Therefore, for long-term monitoring of wall condition, the intensity of the echoes at each antenna orientation is also of interest. The intensity of the return from each wall area is influenced by its roughness and shape.

The dielectric discontinuity between crude oil and rocksalt is calculated from our known values6 to give a microwave power reflection coefficient, Gw^2, near -12 dB $\pm$ 1 dB. The change at the oil-salt interface is assumed to be abrupt on the scale of the 10- to 20-cm wavelengths in the oil. This assumption of abruptness is based on small-diameter leached surfaces observed in the laboratory.

The technology is available for development of a radar tool in the frequency region of 1 to 2 GHz. The microwave components used in this frequency range are available on the commercial market and are well characterized. For example, the maximum power available from power transistors and the best noise figure available with low-noise transistors are known. The approach in this analysis is to derate these quantities by factors of 2 or 3 for the purpose of reliable operation, and then assume extra losses of another factor of 4 or 5 within the antenna array during power transfer out and in.

The measure of tool feasibility being used here is the ratio of the power in the radar signal returned from the wall to the noise power expected in the radar receiver. This is termed the signal-to-noise ratio (S/N) and is calculated for twelve cases in each of the 45 storage caverns, namely, two extremes of wall roughness at two characteristic values of cavern radius at each of three radar frequencies from 1 to 2 GHz.

2 RADAR ANTENNA CHOSEN AND ITS RADIATION PATTERN

Most of the length of the radar tool will be occupied by the antenna. The size of the antenna chosen for this calculation has been described above as being 4.0 meters or 13.3 feet long and the full width permitted by the one-foot diameter. This section presents one example of an antenna configuration of that size which could operate over the range of pressures

required in SPR caverns and be moved through the crude oil efficiently and still act as the large coherent antenna aperture needed to get the narrow beam at the cavern wall. The configuration we choose is a stack of contiguous microwave horns.9

2.1 A Useful Horn Design

One form of microwave horn is a short section of rectangular waveguide flared out smoothly to the desired rectangular opening or aperture. To be useful downhole in a SPR cavern, we suggest the aperture be open to the crude oil and the rear end of the rectangular guide be slotted to permit flow of the oil through the horn during its movements which are required for scanning the wall.

Obtaining efficient energy transfer from the transmitter circuits through each horn to the bulk crude oil and back to the receive circuits are important design steps. Each horn opening is assumed to provide a match to the wave impedance in the oil stored in the cavern. Ring down is assumed to be complete before the end of the round trip transit time of some 300 nanoseconds. Therefore, the same array of horns can be used for receiving.

2.2 Vertical Array of Horns

The antenna is chosen to be a broadside- array of contiguous horn apertures forming effectively one large planar aperture, a rectangle 0.9 foot wide and 13.3 feet long. At one GHz, the array would be composed of forty horns, each 26 cm wide and 10 cm tall, arranged as a stack 20 wavelengths tall. The radiation pattern of such an array when driven coherently with uniform intensity is calculated in Section A3 and has a half-power beam width equal to the expected value of -0.044 radians.[9,10]

Keeping the dimensions of the aperture constant as the design frequency is increased improves the wall resolution. For example, driving a 13.3-foot aperture at 2 GHz narrows the HPBW to 0.022 radians and allows the radar system to resolve wall features that are only 2.2 feet apart at 100-foot radius.

This style of phased array could be used to execute rapid vertical changes in beam direction to angles larger than HPBW. This would decrease the cost of a map by reducing the number of elevation stops needed and by correlating echoes from nearby wall areas in cases of echo fading or abrupt changes in range, without the interruptions required by mechanical repositioning.

2.3 Resolution at Cavern Wall

The wall region contained within HPBWev covers 4.4 feet in depth at 1 GHz and only 2.2 feet at 2 GHz, when the cavern radius is 100 feet. For the sake of this discussion, we assume a truncate beam pattern of uniform illumination intensity inside the HPBW cone and zero intensity outside.

The HPBW in azimuth is calculated for the total aperture width of 10.8 inches for each layer of horn(s). At CR = 100 feet, the wall area contained within the beam solid angle of HPBWaz x HPBWev is 4.4 high and 70 feet wide at 1 GHz as shown in Appendix A in Fig. A3. At 2 GHz, the wall area covered by the half-power cone is 2.2 feet high and 34 feet wide.

If a smooth recess in a cavern wall is illuminated, the central beam will be reflected away from direct return to the antenna and the echo strength reduced sharply. The presence of such a recess would be detected by changes in the radar range when the wall is rough. An axial section of a cavern containing such a narrow beam is shown schematically in Figure 2.3. The figure illustrates the beam impinging on a matte wall patch inside a slight recess in the vertical wall. Identifying the wall contour that produces such localized echo fading is expected to be a frequent task of the radar tool's data processing and scan control systems.

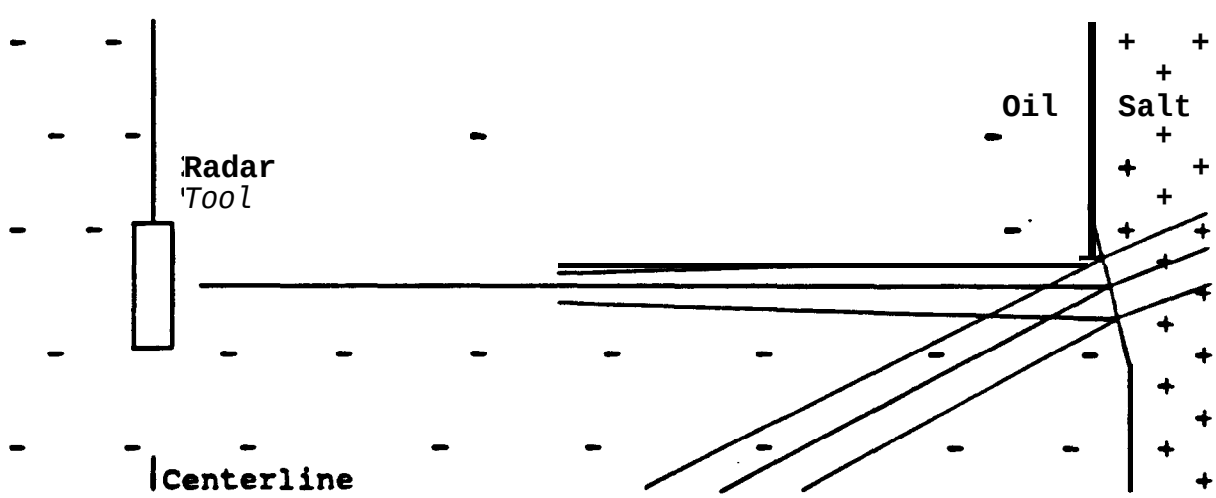

Figure 2.3 Vertical Section of Cavern Containing Radar Array
Beam angle fills 0.044 radians from the 13.3-foot tall antenna array on the cavern centerline.

2.4 Available Loop Sensitivity (ALS)

A critical radar system parameter is the available loop sensitivity (ALS), defined as the ratio of the power transmitted into the oil through a matched antenna aperture to the effective noise power input to the receiver array. Values for ALS are calculated in Appendix A to be 142 dB ± 1 dB on the basis of the conservative assumptions mentioned above. These values are typical of those found in existing high-performance radar systems.

3 ECHO ATTENUATION

Provided the oil within the path of the narrow beam has uniform dielectric permittivity, the power returned to the radar antenna which is located on the cavern centerline is decreased only by the beam spreading calculated above and by the attenuation due to dielectric absorption within the stored oil.[6,8] The power flux in a plane electromagnetic (EM) wave decreases by

27.3 tan6 dB per wavelength.

Tan6 is defined as the ratio of the imaginary part to the real part of the relative permittivity of the oil at the frequency of the wave. Tanδ is called the loss tangent of the oil. The real part is called the dielectric constant of the oil, ε_r'.

3.1 Dielectric Constant and Loss Tangent in SPR Crudes

Recent measurements of microwave transmission through a short oil-filled coaxial holder have supplied values for the dielectric constant and loss tangent of crude oil samples from six SPR caverns over the frequency range from 1 to 10 GHz.[6] The observed tan6 values to be used from reference 4 are listed in Table 5.2.

The microwave values of ε_r' are observed to be constant within three percent from 1 to 10 GHz for any given oil. The spread of ε_r' values among the six crudes measured was 17 percent. We choose a constant value for this study of 2.25 and leave this uncertainty of ± -5 percent in the wavelength to be resolved by later bench measurements.

3.2 Correlation of Loss Tangent with Sulphur Content

The preliminary correlation in Table A2.1 of tan6 with sulphur concentration in the six SPR crudes is assumed to be accurate and, therefore, to apply to the oil in all the SPR caverns. The expression for tan6 given in Section A2 fits the tan6 measured for the six crudes to within ten percent, as shown in Figure A2.2. So the same expression is used to get a $\tan\delta$ value for each of the other SPR caverns. How well the expression fits the oils in the other SPR caverns is not known.

3.3 Echo Attentuation in SPR Caverns

The values of tan6 obtained from the assumed sulphur correlation are then used to calculate the power transmission over the radial distance CR (PT1) with the expression

$$10 \log(PT1) = 27.3 \; Ncr \; \tan 6 \qquad \text{in dB},$$

where Ncr = CR / WL = the number of wavelengths (WL) in the cavern radius, CR. The modified radar equation describes transmission over two radial distances and therefore contains PT1 squared.

The ten percent uncertainty in tan6 and five percent uncertainty in wavelength add to give the uncertainty in PT1. For example, at 1 GHz and at the CReff in SPR Cavern WH112, Ncr = -150 and tan6 = -0.01, giving that transmission coefficient as

$$10 \log(PT1) = -40 \text{ dB} \pm 6 \text{ dB}.$$

PT1 is calculated at each of two radii for each cavern, namely, the minimum cavern radius (CRmin) and an average value called the constructive radius or "the effective cavern radius" (CReff). We use the normal definition of CReff as the square root of the ratio of the cavern volume to π times its height. CRmin is estimated from what is known about the shape of each cavern.[1,2] The values we obtain for PT1 range from a power loss of -10 dB to more than 200 dB depending on the sulphur content of the oil, the cavern dimensions, and the wavelength.

4 CAVERN WALL CONDITION

The cavern wall is an unusual target with an extraordinary radar cross-section. The usual radar equation is modified in Section A4 to express the echo power expected from a cavern wall shaped as a right circular cylinder.

4.1 Salt-Oil Reflection Coefficient

The oil-salt interface is assumed to be an abrupt one on the scale of the radar wavelengths of 10 to 20 cm. Therefore, Eq. A4.1-6 yields the power reflection coefficient, G_w^2, at the interface to be -12.5 dB $\pm$ 1.4 dB.

4.2 Wall Roughness and Contour

Laboratory samples of leached rocksalt have rather smooth surfaces; their roughness scale is approximately one millimeter in a small circular cavern of 10-cm diameter. The actual roughness of SPR cavern walls is unknown.

The roughest surface could have many changes in contour on the scale of several wavelengths as well as roughness down to smaller scales. For this very rough surface, the reflection will be nearly incoherent and almost isotropic into the 2 π solid angle filled with oil.

The smoothest surface we consider is a right circular cylinder that is very rough on a scale smaller than 1/16 wavelength. The reflection is treated as coherent and isotropic. Therefore, it directs all of the reflected waves back toward the original antenna aperture. This is called a matte finish.

5 RADAR S/N CALCULATED FOR SPR CAVERNS

The signal-to-noise ratio to be expected in a SPR cavern (S/N) is the product of the available radar loop sensitivity and echo power return ratio. The latter factor is given by the appropriate form of the radar equation from Section A4. S/N is calculated for each condition in each of the 45 SPR caverns at the three sites.

The S/N ratios, calculated for the 1 GHz conditions, are large for most of the caverns, indicating that definitive radar maps of these walls would be attainable. The S/N values calculated for 1 GHz are shown in Figures 5.1-4 for each of the 45 caverns. Table 5 presents averages of the S/N ratios in the 45 SPR storage caverns that are expected to be greater than unity. For example, in the case of a matte-finish wall shaped as a right circular cylinder, the S/N at the effective radius in each cavern is expected to average -60 dB for 41 of the 45 SPR caverns when the radar is operated at 1 GHz.

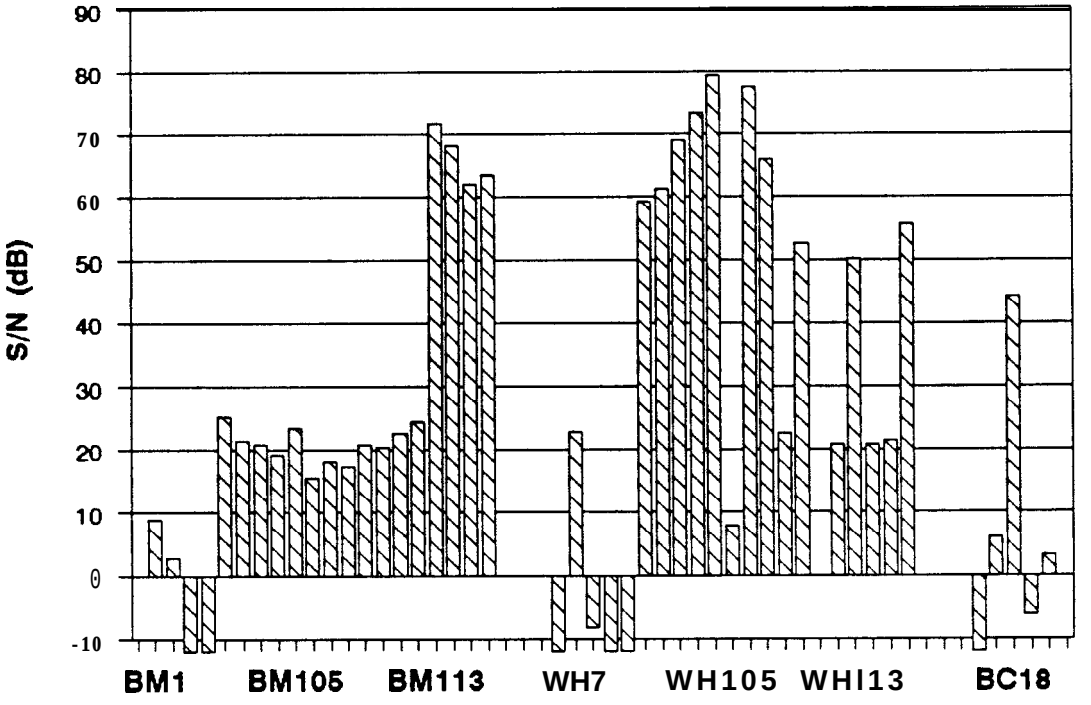

Figure 5.1 Radar S/N expected at 1 GHz in SPR caverns with a very rough wall patch at CReff.

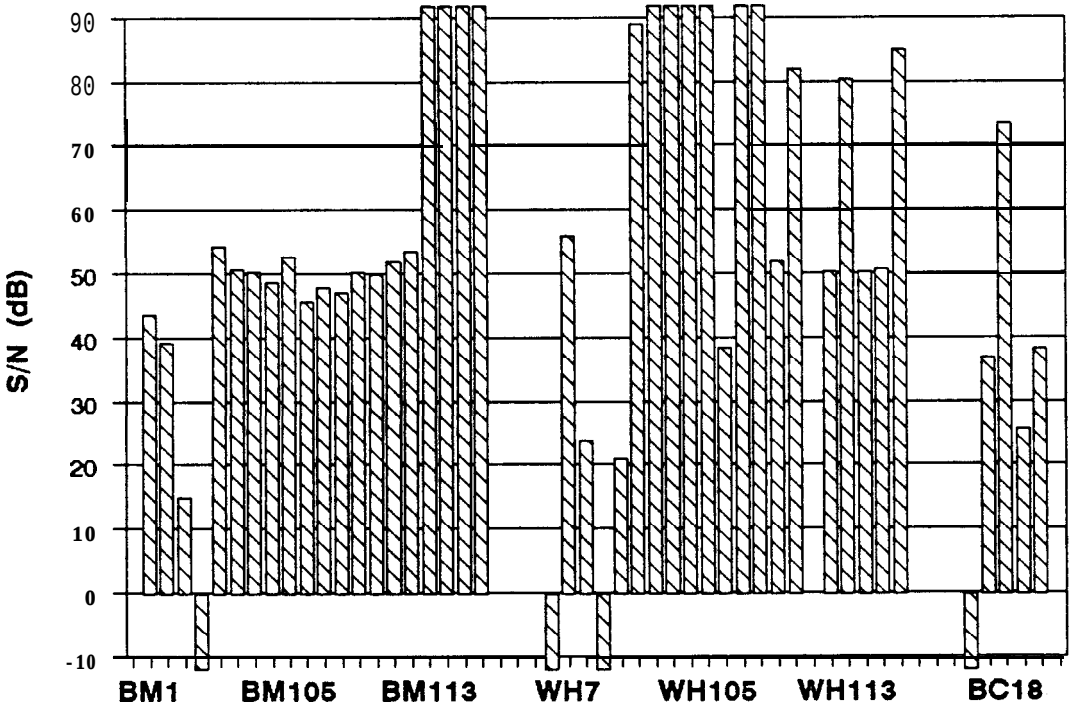

Figure 5.2 Radar S/N expected at 1 GHz in SPR caverns with a matte finish wall patch at CReff.

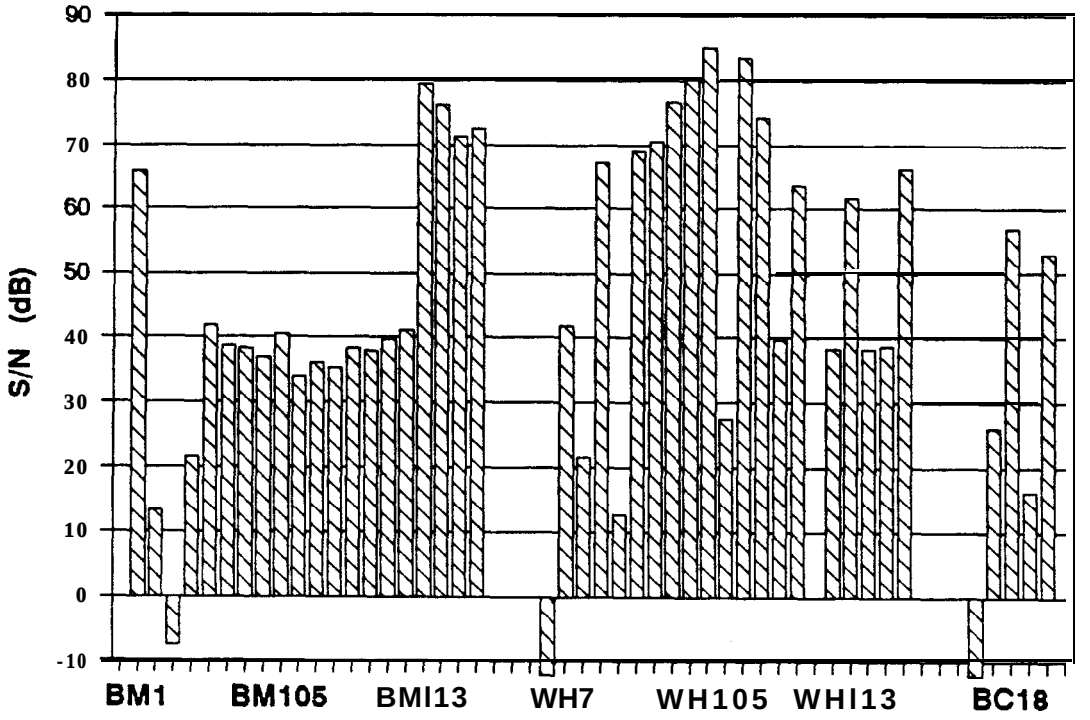

Figure 5.3 Radar S/N expected at 1 GHz in SPR caverns with a very rough wall patch at CRmin.

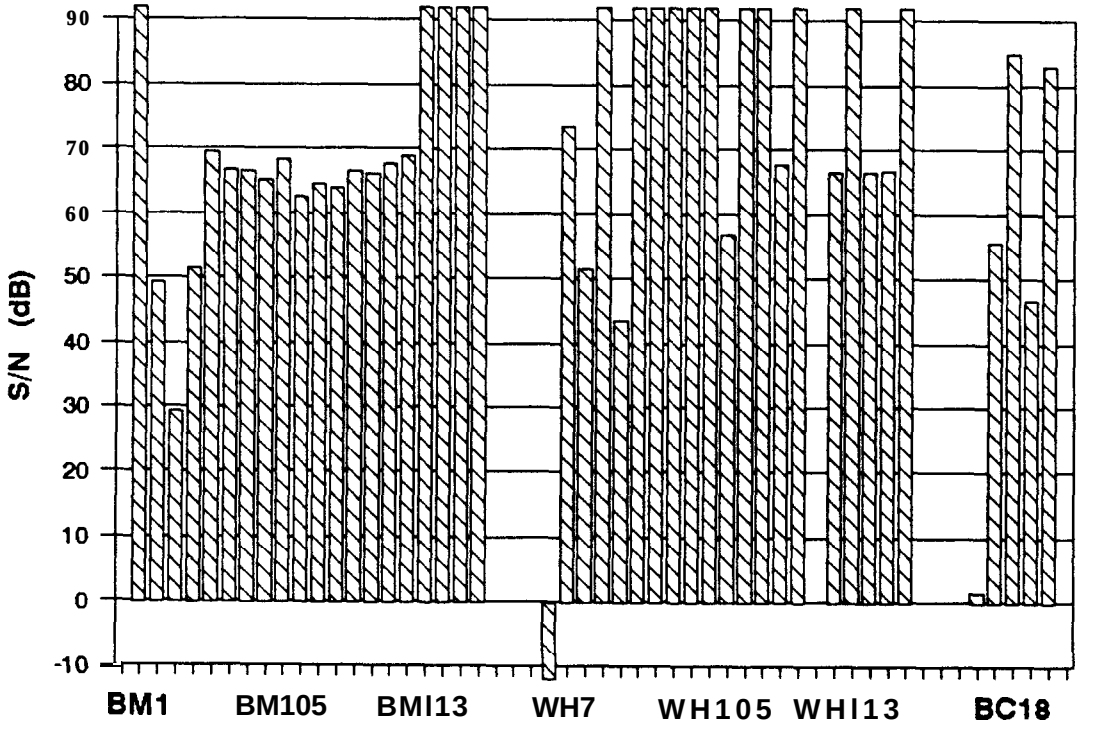

Figure 5.4 Radar S/N expected at 1 GHz in SPR caverns with a matte fi.nish wall patch at CRmin.

The results for the higher frequencies show usable S/N values in fewer of the SPR storage caverns. The S/N values calculated for 1.43 and 2 GHz are displayed in Appendix A in eight bar graphs, Figures A7.1 to A7.8. The cavern labels are again arranged in numerical sequence for each site and a few of the labels are displayed along the bottom of each bar graph. A summary of the results is given in Table 5.

Table 5 Summary of radar S/N predicted for 45 SPR caverns

The S/N values listed in dB are the averages of all the S/N ratios that are greater than unity in each case condition.

Case Conditions:			No. of Caverns:		Average of S/N>1	
Frequency	Range	Roughness	S/N>1	S/N<1	Mean	St. Dev.
1.0 GHz	CReff	rough	37	8	38 dB	24 dB
	CReff	matte	41	4	62 dB	26 dB
	CRmin	rough	42	3	49 dB	21 dB
	CRmin	matte	44	1	75 dB	23 dB
1.4 GHz	CReff	rough	15	30	49 dB	13 dB
	CReff	matte	37	8	41 dB	32 dB
	CRmin	rough	36	9	38 dB	24 dB
	CRmin	matte	42	3	57 dB	27 dB
2.0 GHz	CReff	rough	14	31	34 dB	16 dB
	CReff	matte	15	30	60 dB	18 dB
	CRmin	rough	18	27	45 dB	16 dB
	CRmin	matte	35	10	42 dB	32 dB

6 CONCLUSIONS

Favorable signal-to-noise ratio (S/N) is predicted in most of the SPR caverns for the wall map from a radar tool operating at 1 GHz with a vertical resolution of wall features as close together as five feet and with time resolution capable of measuring the cavern radius to within one foot. The prospects for radar maps to reveal wall features clearly are based on the high value of S/N = -60 dB that is expected on the average from a 1-GHz radar system which is viewing a matte-finish wall patch in each of 41 of the 45 storage caverns considered. For wall features that have very rough surfaces, the prospects are still excellent, since 37 out of the 45 caverns should show a S/N > 1 with an average value of 38 dB.

The prospects of a useful radar map are also high at 1.4 GHz where the wall is smooth enough to have a matte finish. The same 37 caverns would then yield an average S/N ratio of 41 dB.

These calculated S/N ratios have an uncertainty of more than 10 dB due to uncertainties in the dielectric constant and loss tangent values used in these calculations. The accuracy of these predictions can be improved significantly by making microwave bench measurements of the dielectric constants and loss tangents using crude oil samples which are identified by cavern and depth and which have been analyzed for content. Close correlation to the NIPER analysis of the constituents such as sulphur compounds, would then allow NIPER data to predict the microwave properties.

7 RECOMMENDATIONS

The need and criteria for mapping crude oil-filled caverns in this country must necessarily reside with the U.S. Strategic Petroleum Reserve. There is no experience basis from which to estimate the magnitude or frequency of problems an EM tool could address, or the economic value of a tool. The alternative to mapping oil-filled caverns in an emergency is obviously a drawdown (estimated $.25/BBL cost) and sonar through brine. While the technical feasibility of this option is unquestioned, the economic penalty is significant. A radar tool could potentially provide sufficient information to avoid a drawdown.

The predicted feasibililty of a useful radar mapping tool for most of the 45 SPR storage caverns has been established. To define better the feasibility of using radar to map cavern walls, the following studies are needed:

A. Correlate tan6 and ε' at one atmosphere with the NIPER data on chemical content in every cavern of potential interest.

B. Estimate the value of high-resolution wall maps of the oil-filled caverns to the SPR monitoring program. This should include the value of confirming the SNL calculations of creep rate in SPR caverns by measurement of actual creep versus depth.

C. Compare the resolution possible in a map of an SPR oil-filled cavern from linear sonar using a larger transducer with that possible from each of several radar antenna arrays.

D. Consider antenna designs that would swing out to reach -20 wavelengths with a design of the kind described in this report that stays within a one-foot OD during mapping.

E. Document the information from A - D in enough detail to serve as the basis for specifications to be required of a demonstration of cavern wall mapping.

The major assumption to be confirmed by a demonstration of high signal-to-noise ratio of a radar system near 1 GHz is the uniformity of ε' along the 200-foot path of the echoes.

8 ACKNOWLEDGEMENTS

Gratitude is due to J. L. Todd, 6257, who contributed important ideas to this feasibility study, and to the SNL reviewers for several corrections to the calculations and many improvements to the text.

9 REFERENCES

1. D. S. Preece and J. T. Foley, "Long-Term Performance Predictions for Strategic Petroleum Reserve (SPR) Salt Caverns," SAND83-2343, Sandia National Laboratories, Albuquerque, NM.

2. K. L. Biringer, "Strategic Petroleum Reserve Cavern Geotechnical Data Base," SAND84-1500, Sandia National Laboratories, Albuquerque, NM.

3. K. L. Goin and J. T. Neal, "Analysis of Surface Subsidence of the Strategic Petroleum Reserve Crude Oil Storage Sites from December 1982 to January 1988," SAND88-1309, Sandia National Laboratories, Albuquerque, NM.

4. Sonar surveys for SPR caverns at West Hackberry, WH116 on April 25, 1986 and WH114 on February 3, 1987, report "little detail" at sonar ranges near 100 feet in crude oil.

5. Prakla-Seismos GMBH reports of extended sonar range and improved angular resolution in oil-filled storage caverns in West Germany have been published by:

   E. Wierczeyko, "Determination of the Change in Shape and Volume of Salt Cavities During Storage Operation," Sixth International Symposium on Salt, held in Toronto, Canada, on May 26, 1983, and

   E. Nolte, "Survey of Subsurface Oil-Filled Storage Cavities," Fifth Symposium on Salt, held by The Northern Ohio Geological Society in 1980.

6. J. G. Castle, "Microwave Transmission Through SPR Crude Oil Samples from Bayou Choctaw Caverns," SAND88-1895, Sandia National Laboratories, Albuquerque, NM.

7. SPR Drawdown and Distribution Configuration Chart Rev. #25 (4th Quarter '88).

8. J. D. Kraus and K. R. Carver in "Electromagnetics," 2nd Ed., McGraw-Hill Book Co., 1973, ISBN o-07-035396-4. Absorption of electromagnetic energy in terms of the loss tangent is described in terms of 'dielectric hysteresis' on pages 332ff.

9. ibid., Beam patterns from broadside arrays are discussed on pages 633ff.

10. M. I. Skolnik, "Introduction to Radar Systems," 2nd Ed., McGraw-Hill Book Co., 1980, ISBN 0-07-057909-l. Antenna radiation patterns are discussed on pages 224ff.

11. ibid., Skolnik discusses available system gain on page 344.

GLOSSARY OF SYMBOLS IN SAND88-3262

$A_{W1/2}$	area on wall within the half-power directions
Aaz	angle of azimuth in horizontal plane
Aef	effective aperture of antenna; set = AHAW
Aev	angle of elevation (tilt) from horizontal
AH	aperture height of antenna array
ALS	available loop sensitivity
AT1	power transmission from driving transistor to horn
AW	aperture width of antenna
B_n	noise bandwidth of radar system
BM	Bryan Mound SPR site
BC	Bayou Choctaw SPR site
CH	cavern height
CR	cavern radius = range from tool to wall
CReff	effective cavern radius in Volume = A $(CReff)^2$ CH
CRmin	minimum range to a wall feature, e.g., neck in BM1
EM	electromagnetic
dB	decibel, unit of 10 log(power ratio)
ε_r'	dielectric constant; real part of relative permittivity
f	frequency of EM wave radiated by antenna into oil
F_n	noise figure of radar system
G_{DA}	directivity or the directive gain of the antenna
$G_{Dtarget}$	directive gain of the wall target
G_W^2	power reflection coefficient of oil-salt interface
GHz	gigahertz = 1,000,000,000 Hz
HPBWev	half-power beam width in elevation
HPBWaz	half-power beam width in azimuth
K	Boltzmann's constant = 1.38E-23 J/°K
MH	matte finish (surface of wall patch)
[illegible]	megahertz = 1,000,000 Hz
N_h	number of horns in antenna array
Naz	AW / WL, the number of wavelengths in width AW
Ncr	CR / WL, the number of wavelengths in range CR
Nev	AH / WL, the number of wavelengths in height AH
OD	outer diameter
P_{echo}	power incident on antenna aperture within an echo
$P_{noise,eff}$	effective system noise power at input to antenna

GLOSSARY OF SYMBOLS IN **SAND88-3262**
(continued)

P_{tr}	power transmitted from aperture into medium
P_{Winc}	power incident on the cavern wall
P_{Wrefl}	power reflected from the wall
P_{xtr}	available power output from driving transistor
pd	phase difference between center and edge of aperture, viewed along beam
PT1	power transmission coefficient over distance CR
RR	really rough (surface of wall patch)
S(CR,0)	power flux at distance = CR and angle = 0
SPR	U. S. Strategic Petroleum Reserve
SULPHUR	total sulphur concentration in wt percent
S/N	signal-to-noise ratio of radar map
tan6	loss tangent
TO	ambient temperature in °K
TNi	coefficient in expression for tanδ(SULPHUR)
WH	West Hackberry SPR site
WL	wavelength in the crude oil

APPENDIX A: CALCUUTION OF RADAR ECHOES IN SPR CAVERNS

Al SCOPE OF APPENDIX A

Appendix A states in detail the physical basis that we are using to estimate the radar signal-to-noise (S/N) and the accuracy to be expected in mapping SPR cavern walls. Since this is a preliminary study of the feasibility of mapping SPR caverns by a microwave radar tool, the major variables are explored by examining three frequencies, two conditions of wall roughness, and two radius values in each SPR storage cavern at the sites called Bryan Mound (BM), West Hackberry (WH), and Bayou Choctaw (BC). Spreadsheet calculations of S/N for these cases are listed in Appendix B.

The development of the S/N calculation starts in Section A3 with the antenna radiation patterns of the arrays that would operate from within the tool dimensions of one foot diameter and 20 feet long. In Section A4, the radar equation is appropriately modified for the geometry of a radar mapping tool on the centerline of a cavern whose wall is a right circular cylinder. Section A5 evaluates the expected attenuation during the two-way trip in the stored oil. The radar loop sensitivity is stated in Section A6. Section A7 displays the equations for S/N in the several cases and the graphs of S/N for 1.4 and 2 GHz. Since the justification of the expense of radar mapping will rest on an acceptable accuracy of the radar range values, the accuracy available is estimated in the next section before proceeding with the S/N calculations.

A2 ACCURACY EXPECTED IN RADAR RANGE VALUES

The radar range of an echo is the distance the electromagnetic waves travel from the antenna to the target, i.e., the illuminated wall element. The range of a particular echo is calculated as the quotient of a measured travel time divided by a calculated speed of the EM waves. All logging tools assume a uniform medium along the path of the echo. Since SPR oils appear to have a relatively low rate of attenuation, the wave speed is inversely proportional to the square root of the dielectric constant of the oil in the path between the antenna and the wall.

Uncertainties in the radar range are expected to arise from three sources: large-scale wall roughness or strong curvature within the illuminated wall element, uncertainties in the measured time of arrival of the echoes, and uncertainty in the dielectric constant, ε_r'oil. These sources are discussed in Sections A2.1-3.

Some variation of ε_r'oil with depth is expected in some SPR caverns but its size is unknown. If it is proportional to the density change with pressure, then it will be about one percent over the depth of a typical cylindrical cavity. Variations due to temperature and motion of the oil are estimated to be negligible.

A2.1 Range Spread from Wall Roughness

Consider the type of large-scale roughness or wall curvature present when the resolved wall element contains wall patches that are different distances from the antenna. To the extent that these wall patches each produce comparable echo strength, their different ranges will spread out the measured range from a single value to a distribution of observable ranges. Deciphering the distribution in terms of the angular locations of the different wall patches may be possible by correlation of echo profiles from resolved areas that overlap. The task of deciphering this range distribution can be made simpler by shrinking the wall area resolved by a centerline tool. In any case, this source of range change is what makes a map of a cavern wall potentially valuable to the SPR monitoring program.

For this preliminary estimate, we accept the wall resolution attainable from an antenna array that is 10.8 inches wide and 13.3 feet tall. We also use the simplification of the cavern wall being the shape of a right circular cylinder of radius = CR.

A2.2 Echo Arrival Time

The velocity of EM waves in SPR crude oil is 670 million feet/second. To resolve a change in range of one foot requires time resolution for travel of two feet, namely, three nanoseconds. A receiver system with a bandwidth of 50 MHz or greater can resolve two events separated by three ns. Whether the arrival time of an echo is measured by the leading edge of a return pulse or by the frequency shift in the echo from a frequency-swept transmitter, the uncertainty in the time of arrival decreases as the S/N is increased provided the signal bandwidth is wide enough. Assume the time of arrival of a pulse can be observed to within an uncertainty of one-half of the rise time of the receiver. A rise time of -6 ns is available in a receiver with a 50-MHz bandwidth. So the time of arrival of a modest strength echo viewed by a receiver with a 50-MHz bandwidth can be recorded with an uncertainty of -3 ns.

The roundtrip travel over a cavern radius of 100 feet takes 300 nanoseconds. To get the relative uncertainty in the wave speed below 1 %, the dielectric constant of the particular oil in the path of the echo must be known to better than 2 percent. This seems to be no problem since ε' values are reproducible to $\pm$ 0.5 percent during bench measurements on a given crude oil.6

A2.3 Dielectric Constants of SPR Oils

Our recent measurement[6] of the wavelengths in six SPR crudes at room temperature and one atmosphere over the frequency range from 1 to 10 GHz revealed that the wavelengths at 1 GHz in the six different oils are spread over -9 percent. The least observable shift in wavelength was -1 percent. We observed a spread in the wavelengths near 1 GHz which we attribute to a spread of -17 percent in the dielectric constant, ε_r'oil, of the six oils; see Table A5 below.

We have not yet found any correlation of ε_r'oil with chemical constituents listed in the NIPER analysis of these oils. So, we take for the present study the same value of ε_r'oil = 2.25 for each of the SPR caverns and accept an inherent uncertainty of at least $\pm$ -10 percent in the ε_r'oil values therein.

This five percent uncertainty in wavelength and consequently in both range and attenuation, should be reduced to less than one percent by a set of laboratory measurements on SPR oil samples from each cavern of interest. Such data would significantly improve the accuracy of S/N predictions.

A3 RADIATION PATTERN OF ANTENNA ARRAY

We evaluate here the far-field radiation patterns of an array which fills an effective aperture measuring 26 cm wide and 4.0 meters tall in a vertical plane. We assume the array is driven coherently to give uniform phase and intensity across the aperture plane and polarized with the H-plane horizontal. The effective aperture of the array, Aef, is set equal to the actual area.

Separating variables into the azimuth and elevation angles, Aaz and Aev, respectively, the two-dimensional radiation pattern may be written in the usual product form[9,10]

$$G(Aaz,Aev) = Gh(Aaz,0)\ Gh(0,Aev). \qquad [A3\text{-}1]$$

Each horn gain factor, Gh(Ai,O), has the standard form

$$Gh(Ai,O) = (\sin pd)^2 / pd^2, \qquad [A3\text{-}2]$$

where $pd = \pi (AW / WL) \sin(Ai)$ which is equal to one half of the phase difference across the aperture width AW when viewed along Ai.

The bell shape of the well-known sinc^2 function in Eq. A3-2 has two directions in which the power flux is one half of the maximum value at Ai = 0. These two directions are separated by the angle, HPBW, called the half-power beam width.[9,10]

Calculations at f = 1, 1.43, and 2 GHz give, as expected, the values of HPBWi listed in Table A3. The power flux in the first side lobes is down times 20 from the central maximum. Figure A3 shows the azimuthal and elevation views of the radiation pattern generated at a wavelength of 20 cm in the oil. Also shown is the wall area circumscribed by the half-power directions at 1 GHz, a rectangle of height 4.4 feet and width 70 feet.

Table A3 Calculated features of radiation patterns

The antenna array "fills" a vertical aperture 26 cm wide and 20 wavelengths tall in ε_r'oil = 2.25. Angles are in radians.

Frequency GHz	Azimuth Angles HPBWaz	1st Lobe	Elevation Angles HPBWev	1st Lobe	Wavelength cm
1.0	0.70	1.6	0.044	0.072	20
1.43	0.48	0.9	0.044	0.072	14
2.0	0.33	0.6	0.044	0.072	10

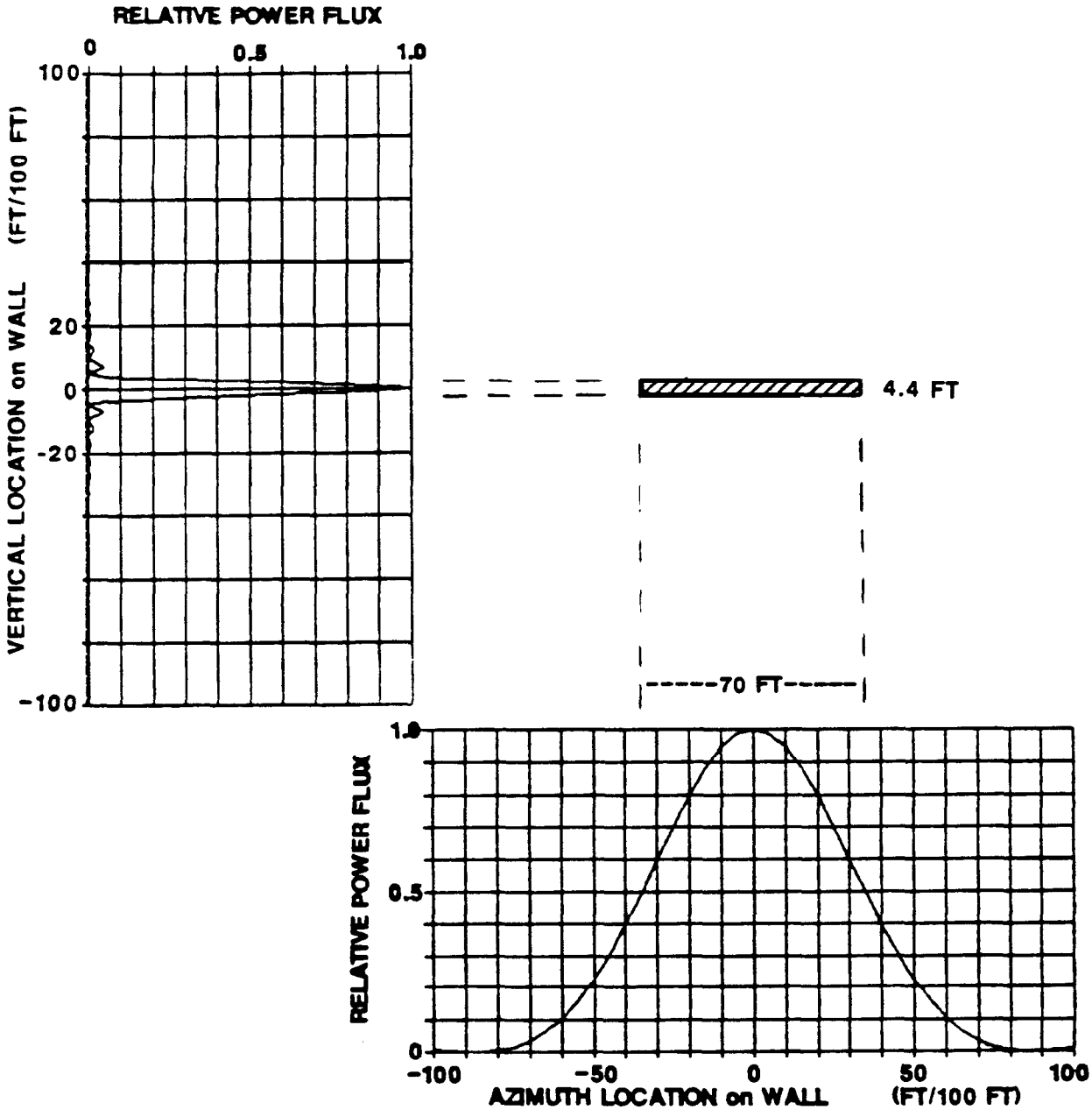

Figure A3 Antenna radiation pattern for 1 GHz in SPR oil. Shaded rectangle represents that wall area, 4.4 x 70 feet, inside the cone of half-power directions. Effective aperture of antenna is 0.87 foot wide and 13.3 feet tall, driven with uniform phase and amplitude at the wavelength of 2/3 foot.

4 THE RADAR EQUATION FOR CAVERN MAPPING

In radar, the ease of detecting an echo is measured by the ratio of the power in an echo to the power received in the noise background, called the radar system's signal-to-noise ratio (S/N). S/N is calculated from the definition

$$S/N = \frac{\text{Power in echo}}{\text{Effective noise power into antenna}} \qquad [A4\text{-}1]$$

For example, when the S/N is 30 dB, the echo power is 1000 times the noise background and is easily detected above the noise. With such high S/N, deciphering the observed range distribution should be successful. The limit of detection is often considered to be when echo power is equal to rms noise power i.e., S/N = 0 dB.

A4.1 Modifying the Radar Equation for Wall Mapping

The power expected in a radar echo for a small target at a particular range from the antenna is often stated as a fraction of the transmitted power by an expression called the radar equation.[9,10] The usual radar equation contains a factor called the "radar cross-section" of the target. In this study, the whole cavern wall is the target and we approximate that target to be only the portion of the wall inside the half-power cone, as described above in Section A3.

In this section, the radar equation is adapted to wall mapping by using simplified geometric arguments related to the different cases of wall roughness to calculate the echo power returned to the centerline antenna. Following Skolnik on page 3 and Kraus and Carver on page 696, we note that the power density, S, after traveling the distance to the wall, CR, in a lossless medium from an antenna with directive gain = G_{DA} and power transmitted into the medium = P,,, is written

$$S(CR,0)_{\text{zero loss}} = \frac{P_{tr}\, G_{DA}}{4\,\pi\, CR^2} \qquad [A4.1\text{-}1]$$

The attenuation due to the loss tangent of the oil over the distance to the wall may be represented by the power transmission coefficient (PT1). In the approximation of "the cavern radius," CR, being much larger than the dimensions of the antenna aperture and much larger than the variation in actual distance to the wall from this "cavern radius," PT1 may be expressed in terms of a single value for the distance; we use CR. PT1 also depends on the loss tangent of the oil and is specified in full in Section A5. The power density arriving at the cavern wall is reduced to

$$S(CR,O) = \frac{P_{tr}\ G_{DA}\ PT1}{4\ \pi\ CR^2} \qquad [A4.1\text{-}2]$$

Along other directions of propagation away from this central one, the power density in the antenna radiation pattern at the wall decreases due to interference from the phase difference across the antenna aperture, as calculated in Section A3.

A4.1.1 Directivity of Antenna

The directive gain or directivity of an antenna, G_{DA}, is the ratio of power density on beam center to the average power density over all directions. It involves the effective aperture of the antenna in the forma

$$G_{DA} = \frac{4\ \pi\ Aef}{WL^2}\ . \qquad [A4.1\text{-}3]$$

For a rectangular antenna aperture that is driven with uniform phase and amplitude so that each HPBW -- 0.88 times the reciprocal of the number of wavelengths across the aperture, the directive gain is

$$G_{DA} = 4\ \pi\ Nev\ Naz. \qquad [A4.1\text{-}4]$$

For example in Section A3 above, the antenna array whose effective aperture is 26 cm wide and 20 wavelengths tall has

G_{DA} = -300 at 1 GHz in SPR oil.

A4.1.2 Truncate Pattern of Incident Pover Flux

In the main lobe of every radiation pattern, the directions for which the power density is half the maximum value form a cone. In the present treatment of wall reflections, the wall inside the half-power cone is the resolution element of wall area, $A_{W1/2}$.

The usual first approximation replaces the actual radiation pattern by the truncate distribution in which the power density S is the constant maximum value, S(CR, 0), over this element of area, $A_{W1/2}$, and S(CR, wide angle) = 0 outside the half-power cone. Therefore, the power incident on this target area, P_{Winc}, is the product of S(CR, 0) times $A_{W1/2}$. By substitution from the equations above, we get the Friis transmission equation

$$\frac{P_{Winc}}{P_{tr}} = (0.88)^2 \; PT1 = 0.77 \; PT1 \; . \qquad [A4.1\text{-}5]$$

The rectangle in Figure A3 is an example of the wall element on which this power is incident.

One indication of the utility of this approximation is given by the peak intensities calculated above for the side lobes of the antenna array. When the S/N is high, the radar system will be able to 'resolve' signals from small portions of $A_{W1/2}$.

A4.1.3 Power Reradiated from Wall

The usual reradiation from a small target into the solid angle of 4 A is replaced by the specific reradiation pattern expected from the illuminated wall element which has a given shape and roughness. For each wall condition, the power reflection coefficient, Gw^2, due to the abrupt discontinuity of the dielectric constant from oil to salt is assumed to be the square of

$$G_W = \frac{\varepsilon_r'^{\,0.5}_{salt} - \varepsilon_r'^{\,0.5}_{oil}}{\varepsilon_r'^{\,0.5}_{salt} + \varepsilon_r'^{\,0.5}_{oil}} \; . \qquad [A4.1\text{-}6]$$

With our model value of $\varepsilon_r'oil = 2.25$ and reference value of $\varepsilon_r'salt = 6.12$, $Gw^2 = -12.5$ dB. The spread in $\varepsilon_r'oil$ observed in six crudes from SPR caverns gives a spread in Gw^2 of $\pm$ 1.4 dB.

The total power reflected from $A_{W1/2}$ is

$$P_{Wrefl} = P_{Winc} \; G_W^2 = 0.77 \; PT1 \; G_W^2 \; P_{tr} \; . \qquad [A4.1\text{-}7]$$

The directive gain in this reradiation from the target portion of the wall is labelled $G_{Dtarget}$. Using the same reasoning as that behind Eq. A4.1-2, the power density back at the antenna is

$$S(2\ CR,0) = \frac{P_{Wrefl} \; PT1 \; G_{Dtarget}}{4 \; A \; CR^2} \qquad [A4.1\text{-}8]$$

A4.1.4 The Modified Radar Equation

The total power incident on the antenna, P_{echo}, in our approximation, is the product $P_{echo} = S(2\ CR,0)\ Aef$. Substitution gives the radar equation modified for mapping cylindrical caverns of circular section as

$$\frac{P_{echo}}{P_{tr}} = 0.77 \; (PT1)^2 \; G_W^{\;2} \; G_{Dtarget} \; \frac{Nev \; Naz}{4 \; \pi \; Ncr^2} \qquad [A4.1\text{-}9]$$

where Nev, Naz, and Ncr are the numbers of wavelengths within the dimensions AH, AW, and CR, respectively. Expressions for $G_{Dtarget}$ are derived in this section for two wall conditions. The general definition of directivity is used for each case.

A4.2 Radar Equation for Matte Finish Wall Condition

When the cavern wall is smooth on the scale of one foot but very rough on a scale much less than one quarter wavelength, the reflection takes the form of reradiation isotropically into the 2π steradians filled with oil. With the wall being a circular cylinder and the radar tool at its center, every small element of wall area is being driven coherently in phase in this Fraunhofer region. Therefore, the reradiation is focussed back onto the antenna aperture and the power density near the antenna is

$$S(2\ CR,O,MF) = \frac{P_{Wrefl} \; PT1}{Aef} \qquad [A4.2\text{-}1]$$

By the form of Eq. 4.1-2, the maximum power density is also

$$S(2\ CR,0,MF) = \frac{P_{Wrefl}\ PT1}{4\ \pi\ CR^2}\ G_{Dtarget}(MF)\ . \qquad [A4.2\text{-}2]$$

Dividing gives the directive gain from the matte finish wall as

$$G_{Dtarget}(MF) = \frac{4\ \pi\ CR^2}{Aef} = \frac{4\ \pi\ Ncr^2}{Nev\ Naz}\ . \qquad [A4.2\text{-}3]$$

After substitution of $G_{Dtarget}(MF)$ into Eq. A4.1-9, the radar equation for the case of a matte finish wall becomes

$$\frac{P_{echo}(MF)}{P_{tr}} = 0.77\ (PT1)^2\ G_W^2\ . \qquad [A4.2\text{-}4]$$

The simplicity of this equation is the result of reciprocity when the matte finish scatters isotropically but is coherently driven in phase.

A4.3 Radar Equation for Very Rough Wall Condition

Consider the wall to be rough on the scale of one wavelength or larger. For a target area as large as 6 x 100 wavelengths, the reflection can be treated as reradiation with the small wall elements being driven in random phase.

The resulting directive gain is two if the energy stays in the oil, but only one if the energy is spread isotropically over all directions. Using the lower value, $G_{Dtarget}(RR) = -1$.

The radar equation for such a very rough wall is

$$\frac{P_{echo}(VR)}{P_{tr}} = 0.77\ (PT1)^2\ G_W^2\ \frac{Nev\ Naz}{Ncr^2}\ , \qquad [A4.3\text{-}1]$$

The echo strength in this case of incoherent scattering by the wall is reduced by a sizable factor, namely, Nev Naz / Ncr_2. For the array being used in this study at CR ~ 100 feet, this factor is ~1/1,000 or --30 dB.

A5 ATTENUATION IN SPR CRUDE OILS

To estimate loss tangents in the other SPR oils, we rely on the accurate values of tan6 we have recently observed in six SPR wellhead oil samples of uncertain chemical concentrations. We assume the total sulphur concentration (SULPHUR) listed by NIPER for January 1988 downhole is the same as the SULPHUR in the well- head samples of March 1988 from Bayou Choctaw and of several years ago from West Hackberry.[7] We ignore the apparent dependence of tanδ on specific sulphur compounds6 and assume a one-to-one correlation between tan6 and SULPHUR exists and is given by Eq. A5.2-1 below. Tanδ values to be expected from this simple model are then calculated for each cavern at BM, WH, and BC.

A5.1 Loss Tangents Observed for Six SPR Caverns

We have recently described6 observations of microwave transmission through samples of crude oil from SPR in terms of effective values of loss tangent. A few of those values are listed in Table A5.1, along with the total sulphur concentration, SULPHUR, in weight percent. The unusual decrease in tan6 with increasing frequency is evident in the table.

Table AS.1 Microwave loss tangents, dielectric constants, and sulphur concentrations observed in SPR crude oils

Samples were taken from wellheads at BC in March 1988 and at WH several years ago. BC samples for chemistry by NIPER were taken at several depths in January 1988. SULPHUR is not reported for Bayou Choctaw Cavern 17.

Sample	Microwave Loss Tangent 1 GHz	2 GHz	4 GHz	Dielectric Constant	SULPHUR wt %
BC15	0.0090	0.0086	0.0067	2.22	1.56
BC17	0.0081	0.0078	0.0065	2.19	
BC18	0.0067	0.0064	0.0050	2.17	0.41
BC19	0.0103	0.0095	0.0075	2.28	1.61
BC20	0.0064	0.0058	0.0045	2.18	0.34
WH105	0.0026	0.0026	0.0024	2.335	0.20

The tentative model proposed in Reference 6 for the unusual frequency dependence of these loss tangents predicts little change in loss tangent below 1 GHz. The extent of decrease above 1 GHz depends strongly on the sulphur compounds present. The identity of the specific sulphur compounds which produce these losses remains to be established.

A5.2 An Expression for Tanδ versus SULPHUR

The observed values for tan6 are fitted well by the expression

$$\tan 6 = TNi(1 - \exp(-8\ SULPHUR^2)) , \qquad [A5.2\text{-}1]$$

where TNi = 0.0097 at 1 GHz, 0.0090 at 2 GHz, and 0.0070 at 4 GHz. Deviations of tan6 by Eq. A5.2-1 from the observed values in Table A5.2 are all less than 10 %. Figure A5.2 shows the relative deviations at 1 GHz.

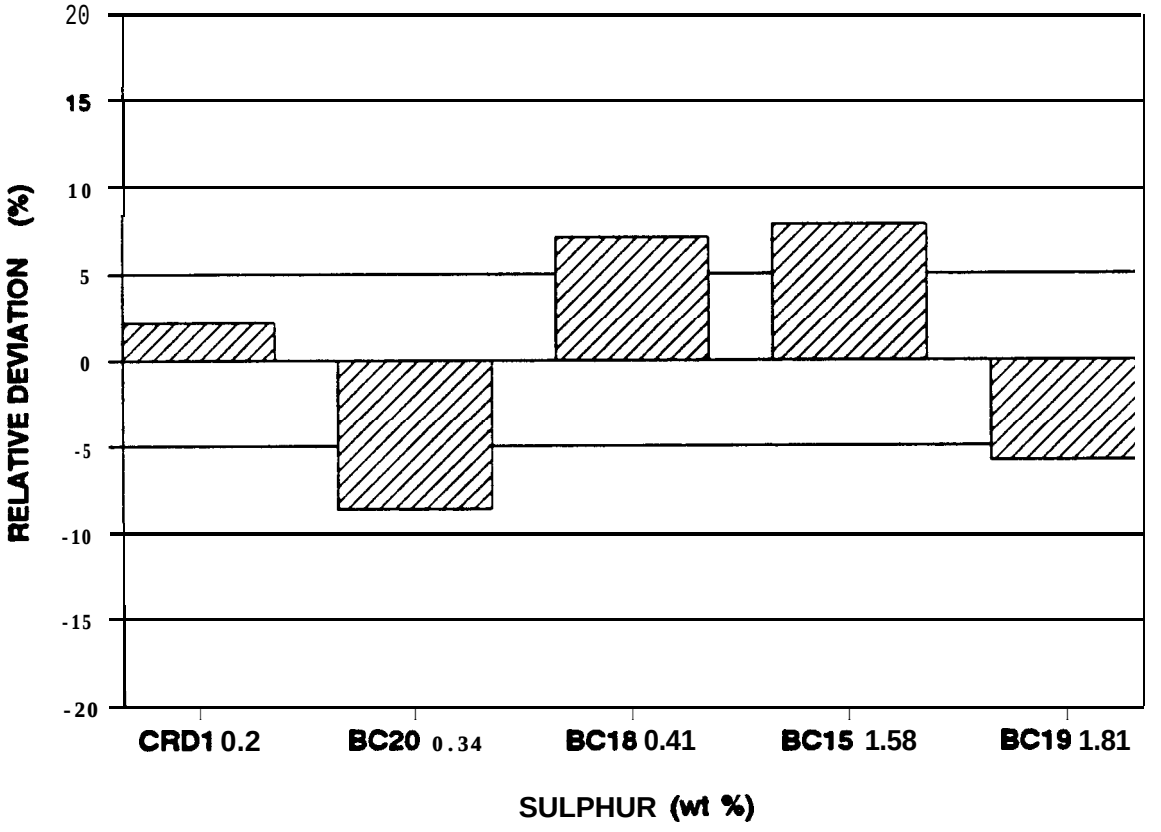

Figure A5.2 Fit of expression for tanδ to observed tan6. Relative deviations of Eq. 5.2-l values from the measured data in Table 5.1 are plotted for the case of f = 1 GHz.

Equation A5.2-1 is used to calculate an approximate value for the loss tangent of the oil in each SPR cavern. These tan6 values are listed and used in the spreadsheet calculation in Appendix B.

A5.3 Power Transmission of Cavern Oil

The one-way power transmission coefficient, **PT1**, in a given oil is fixed for a given wavelength **(WL)** and a given distance to the wall. The fraction of microwave power transmitted over a distance of N wavelengths in a uniform medium is given **by**[6]

$$T^2 = \exp(2 \pi N \tan 6) . \qquad [A5.3\text{-}1]$$

An equivalent statement is that the fractional power flux remaining in a plane wave after travelling a distance = CR is

$$10 \log(PT1) = 27.3 \, Ncr \tan 6 \quad \text{in dB}, \qquad [A5.3\text{-}2]$$

where Ncr = CR / WL. Doubling the expression in Eq. **A5.3-2** gives **(PT1)**^{2} in the radar equations stated above.

The values of the radial distance between radar tool and cavern wall, CR, chosen for these calculations are characteristic ones for each cavern. In the first case, CR = the effective cavern radius (CReff), which is defined as the square root of the ratio of the cavern volume to π times the cavern height. CReff represents the radar range typical of many portions of the wall in most caverns. In the second case, CR = the minimum cavern radius **(CRmin)** which we set equal to 0.8 times CReff if the cavern is carrot-shaped or, in odd-shaped caverns, equal to the minimum distance to some special feature like the neck in cavern **WH9**. The **CRmin** case illustrates how much stronger the radar signals become when the wall is closer to the radar tool.

A6 AVAILABLE LOOP SENSITIVITY FOR RADAR TOOL

The available loop sensitivity **(ALS)** for a radar system, also known as its available gain, is the ratio of peak power out of the antenna to the lowest power input to the antenna.11 Using for the latter the effective thermal noise power into the antenna, $P_{noise.eff}$, we write

$$ALS = \frac{P_{tr}}{P_{noise,eff}} , \qquad [A6\text{-}1]$$

where $P_{noise,eff} = k \, T_o \, F_n \, B_n$ in watts,
$k \, T_o = 4.1E\text{-}21$ watts/Hz at 300 "K,
F_n is the noise figure of the radar receiver with antenna, and B_n is the effective noise bandwidth in Hz.

The array consists of N_h horns, each driven by a power transistor whose maximum output power is P_{xtr}. Defining the power transmission coefficient from the driving transistor to the antenna aperture as AT1, the available gain may be written as

$$ALS = \frac{P_{xtr}\ N_h\ AT1}{(4.1E\text{-}21)\ F_n\ B_n}\ . \qquad [A6\text{-}2]$$

Values for each of these factors are discussed and selected in this section.

The signal bandwidth for each echo is required to be -50 MHz in order to get the range resolution of -one foot from the discussion in Section A3 above. We assume the data are gathered using a signal bandwidth of 50 MHz for each echo. The radar system needs to have the capability of integration of a selected set of echoes. Usually these echoes will be consecutive ones from the same direction. Frequently the echos selected will bear on the identity of source of echo fading. To reduce Bn from 50 MHz to -20 MHz, for example, it should be sufficient to add the wave patterns of eight echoes. This could easily be done in an integration time consistent with obtaining a wall map in a typical SPR cavern within 24 hours of scanning. To be conservative, the present calculations use the full 50 MHz as B,.

Noise figures near 1.5 are available in receivers using silicon transistors at these frequencies while operating at or near room temperature. For this calculation, we use NF = 4.5 to allow for noise generation in the horns and in the array waveguide phase controls. The related quantity, AT1, is set to 0.2, allowing the use of loss up to 7 dB to control the 40-horn array.

P_{xtr}, the cw power available from a single power transistor into a matched load, is 100 watts at 1 GHz and is 30 watts at 2 GHz. Derating a factor of four will improve transistor life. So we set P_{xtr} = 25 watts at 1 GHz and 8 watts at 2 GHz. Therefore, in the present calculation, the forty-horn array at 1 GHz has a total output power during a short pulse equal to 200 watts into the oil.

The available loop sensitivity for this set of system parameters is therefore

ALS = 143 dB at 1 GHz, 142 dB at 1.4 GHz, and 141 at 2 GHz.

A7 EXPECTED SIGNAL-TO-NOISE (S/N)

The S/N to be expected within a radar map of each SPR cavern wall is therefore obtained from Eqs. **A4-1** and **A6-1** as the product

$$S/N = ALS \frac{P_{echo}}{P_{tr}} \qquad [A7\text{-}1]$$

This power ratio is given by the radar equation for each case.

Case **MF** - For a matte finish cylindrical cavern wall, substitution from Eq. A4.2-1 gives

$$S/N(MF) = 0.77\ ALS\ (PT1)^2\ G_W^2\ . \qquad [A7\text{-}2]$$

For a mirrored wall, the particular dimensions in this study give a S/N value approximately the same as from Eq. A7-2.

Case **VR** - For a very rough wall, Eq. **A4.3-1** produces

$$S/N(VR) = 0.77\ ALS\ (PT1)^2\ G_W^2\ \frac{Nev\ Naz}{Ncr^2} \qquad [A7\text{-}3]$$

Values of S/N for these cases are calculated in Appendix B. Each of the oil-filled SPR caverns at Bayou Choctaw, Bryan Mound, and West Hackberry uses one row of that spreadsheet.

The S/N values calculated at 1 **GHz** from Eqs. **A7-2** and **A7-3** are shown in the bar graphs, Figures 5.1-4. These values are summarized in Table 5. The effect of incoherence is shown by the values for the very rough case being nearly 30 db lower than for the matte finish case. The S/N at 1 **GHz** is high at **CReff** and it gets better by some 20 to 50 **dB** at **CRmin. It** is clear that excellent signal-to-noise is available at 1 **GHz** in all but a very few of the SPR caverns at the BC, BM, and WH sites.

The S/N values calculated for 1.43 **GHz** and for 2 **GHz** from the same two equations are shown in the eight bar graphs in this section. The same dependence on CR and incoherence is seen as at one **GHz.** Operation at 1.4 **GHz** would be satisfactory in all but ten or 12 of the 45 caverns, if the walls have a matte finish and are shaped in the form of a right circular cylinder. Clearly, if only one radar frequency will be available in the mapping tool, 1 **GHz** is strongly preferred over 1.4 **GHz** or 2 **GHz.**

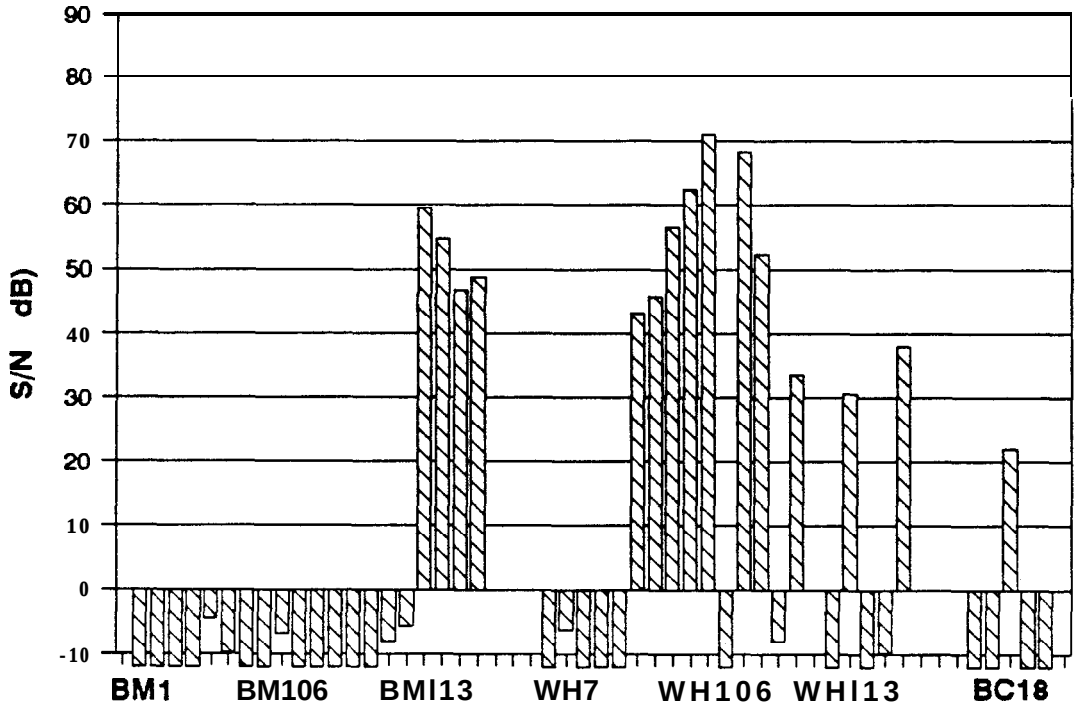

Figure A7.1 Radar S/N expected at 1.4 GHz in SPR caverns with a very rough wall patch at CReff.

Figure A7.2 Radar S/N expected at 1.4 GHz in SPR caverns with a matte wall patch at CReff.

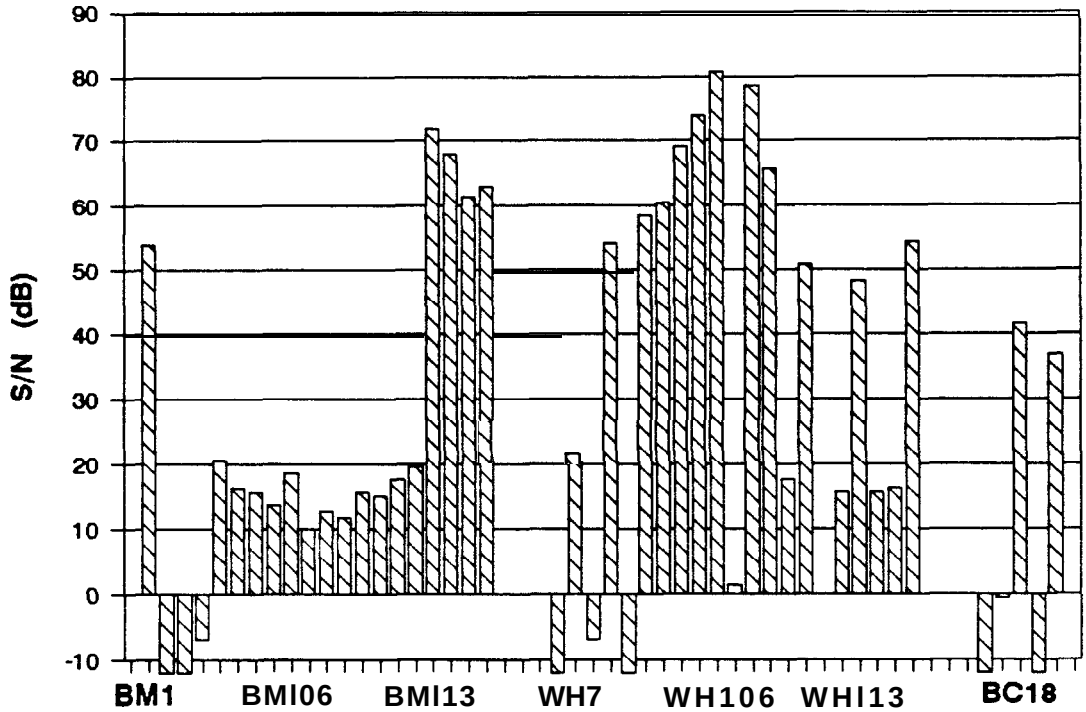

Figure A7.3 Radar S/N expected at 1.4 GHz in SPR caverns with a very rough wall patch at CRmin.

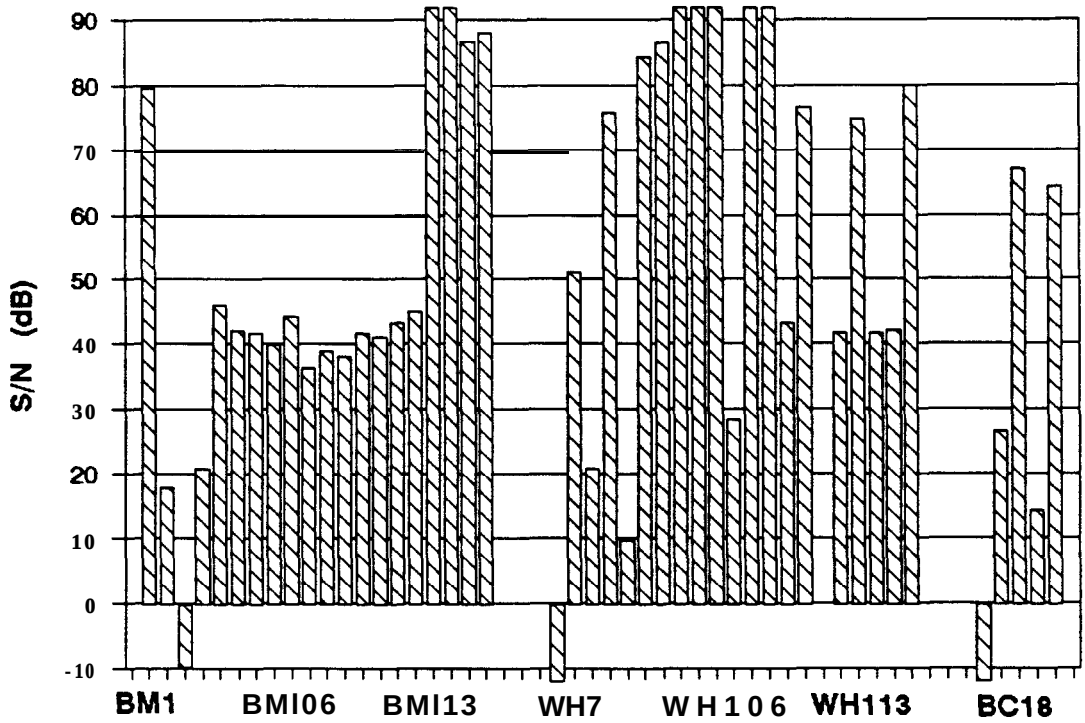

Figure A7.4 Radar S/N expected at 1.4 GHz in SPR caverns with a matte wall patch at CRmin.

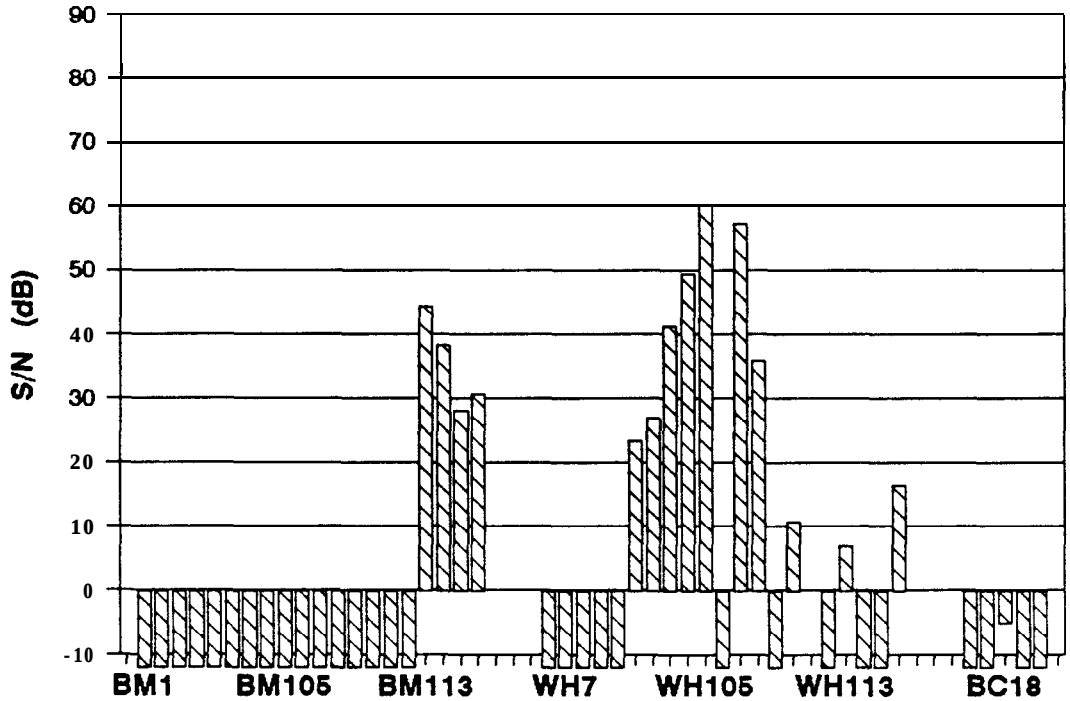

Figure A7.5 Radar S/N expected at 2 GHz in SPR caverns with a very rough wall patch at CReff.

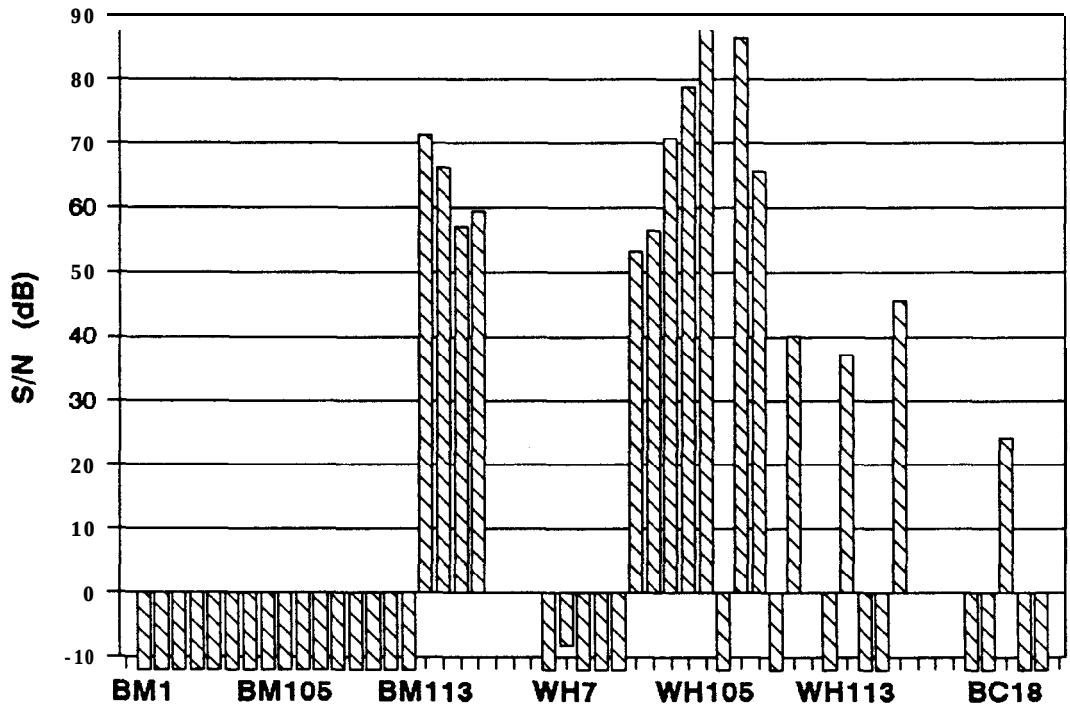

Figure A7.6 Radar S/N expected at 2 GHz in SPR caverns with a matte wall patch at CReff.

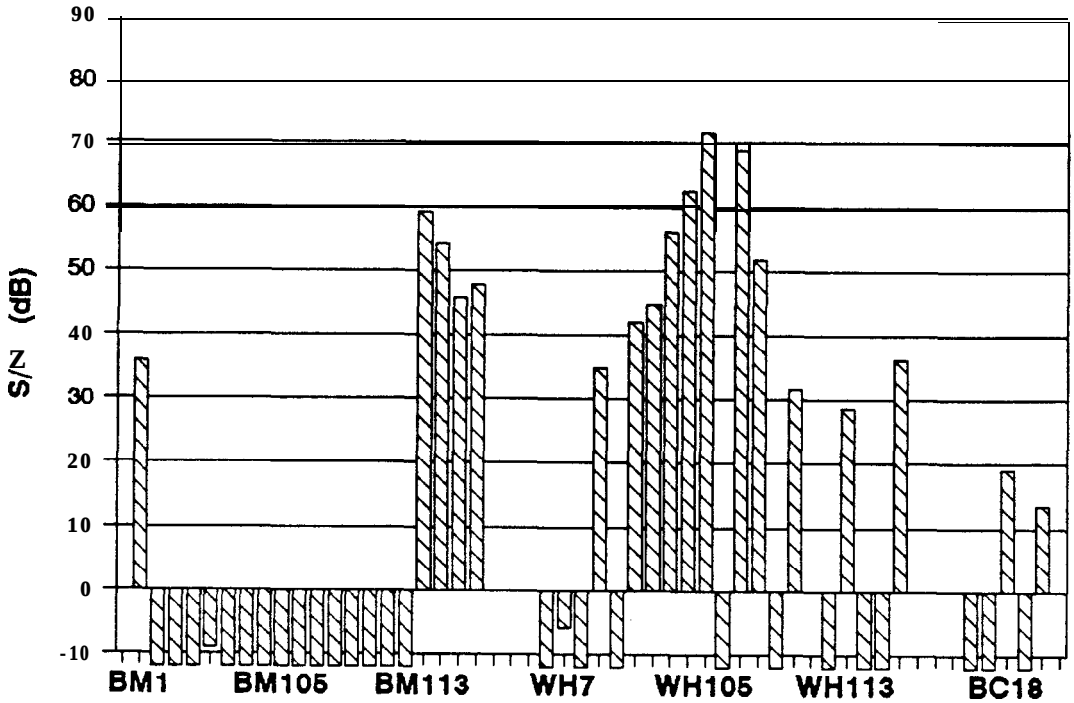

Figure A7.7 Radar S/N expected at 2 GHz in SPR caverns with a very rough wall patch at CRmin.

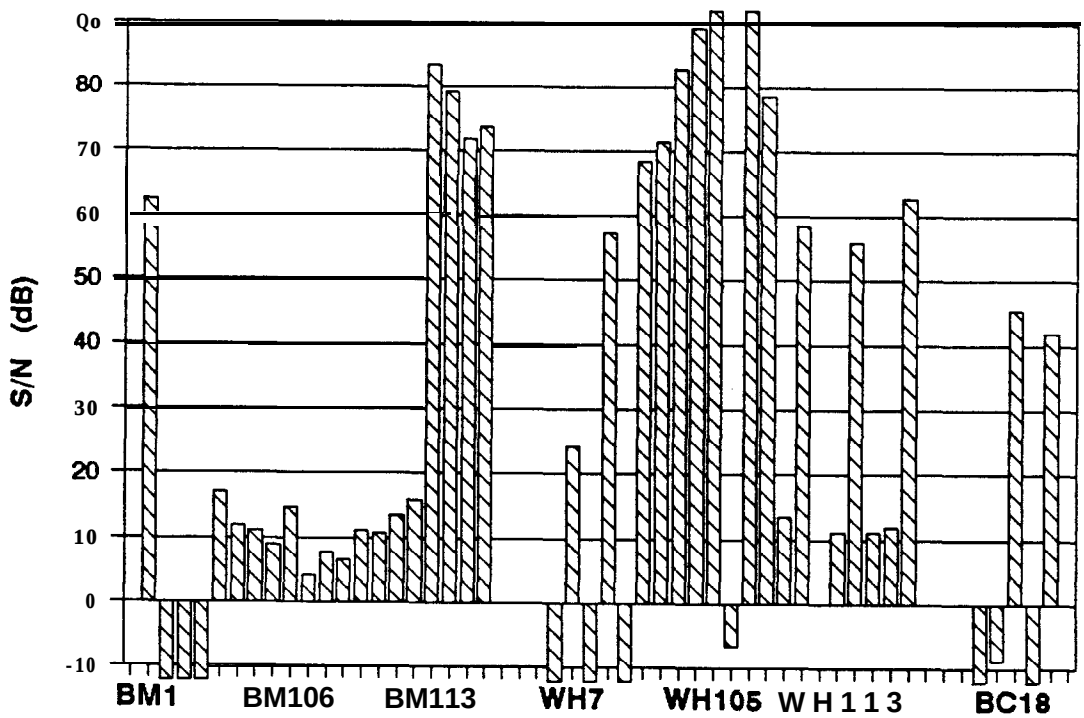

Figure A7.8 Radar S/N expected at 2 GHz in SPR caverns with a matte wall patch at CRmin.

APPENDIX B SPREADSHEET LISTING OF S/N FOR SPR CAVERNS

This appendix presents a two-page table containing the radii and loss values used to characterize each of the 45 SPR caverns and the radar signal-to-noise (S/N) calculated for each of the twelve survey cases as discussed in the text and in Appendix A. Each row in the table represents one SPR cavern, as **labelled** in the leftmost column on each page.

The columns C to H contain SPR inventory and cavern dimension values. Columns J, K, 6 L hold the tan6 values calculated from the SULPHUR values in column F. Columns 0 - T list the S/N calculated for the distance to the wall being the effective cavern radius, **CReff**; columns U - Z, for a minimum distance, **CRmin**.

A	B	c	D	E	F	G	H	I	J	K	L	M
SPR		CReff	CRmin	Inventory	9/30/88		Casing		tandoil	tandoil	tandoil	
Cavern				Oil	SULPHUR		I.D.		f-1.0	f-1.43	f=2.0	
Label		(feet)	(feet)	(MMbbl)	(wt %)		(in)					
Bryan Mound Site:												
BM1		109	80	7.02	0.33		13.3		0.0056	0.0055	0.0052	
BM2		225	200	5.92	0.30		13.3		0.0050	0.0048	0.0046	
BM4		251	220	20.39	0.33		13.3		0.0056	0.0055	0.0052	
BM5		243	100	19.18	1.60	approx.	13.3		0.0097	0.0094	0.0090	
BM101		97	77	10.86	1.35		16.0		0.0097	0.0094	0.0090	
BM102		101	81	10.92	1.38		16.0		0.0097	0.0094	0.0090	
BM103		102	81	10.40	1.51		16.0		0.0097	0.0094	0.0090	
EM104		104	83	10.49	1.62		13.3		0.0097	0.0094	0.0090	
BM105		99	79	10.93	1.51		16.0		0.0097	0.0094	0.0090	
BM106		108	86	11.06	3.25		13.3		0.0097	0.0094	0.0090	
BM107		105	04	11.14	1.30		13.3		0.0097	0.0094	0.0090	
BM108		106	84	11.41	1.47		13.3		0.0097	0.0094	0.0090	
BM109		102	81	10.62	1.53		13.3		0.0097	0.0094	0.0090	
BM110		102	82	10.42	1.57		13.3		0.0097	0.0094	0.0090	
BM111		100	80	10.69	1.43		16.0		0.0097	0.0094	0.0090	
BM112		90	70	10.50	1.55		16.0		0.0097	0.0094	0.0090	
BM113		79	63	4.40	0.30	approx.	13.3		0.0050	0.0048	0.0046	
BM114		86	60	7.17	0.30	approx.	13.3		0.0050	0.0048	0.0046	
BM115		98	70	8.96	0.30	approx.	13.3		0.0050	0.0048	0.0046	
BM116		95	76	9.73	0.30	approx.	13.3		0.0050	0.0048	0.0046	
West Hackberry Site:												
WH6		311	240	7.51	1.52		13.3		0.0097	0.0094	0.0090	
WH7		157	120	12.53	0.34		13.3		0.0059	0.0057	0.0054	
WH8		135	100	9.97	1.52		13.3		0.0097	0.0094	0.0090	
WH9		221	50	9.38	1.53		13.3		0.0097	0.0094	0.0090	
WH11		139	110	0.35	1.47		13.3		0.0097	0.0094	0.0090	
WH101		103	82	10.44	0.30		20.0		0.0050	0.0048	0.0046	
WE102		103	02	10.75	0.29		20.0		0.0048	0.0046	0.0044	
WH103		104	83	10.15	0.25		20.0		0.0038	0.0037	0.0035	
WE104		103	02	11.13	0.23		20.0		0.0033	0.0032	0.0031	
WH105		102	81	10.67	0.20		20.0		0.0027	0.0026	0.0025	
WH106		117	93	10.00	1.37		20.0		0.0097	0.0094	0.0090	
WH107		102	81	11.92	0.21		20.0		0.0029	0.0028	0.0027	
WH108		106	85	6.14	0.26		20.0		0.0041	0.0039	0.0038	
WH109		100	80	8.07	1.23		20.0		0.0097	0.0094	0.0090	
WH110		102	02	10.29	0.34		20.0		0.0059	0.0057	0.0054	
WH112		102	81	9.73	1.31		20.0		0.0097	0.0094	0.0090	
wH113		110	88	4.67	0.33		20.0		0.0056	0.0055	0.0052	
WH114		102	81	8.66	1.31		20.0		0.0097	0.0094	0.0090	
WH115		101	81	6.02	1.35		20.0		0.0097	0.0094	0.0090	
WH116		100	80	10.61	0.33		20.0		0.0056	0.0055	0.0052	
Bayou Choctaw Site:												
BC15		204	163	16.14	1.55		13.3		0.0097	0.0094	0.0090	
BC17		119	95	7.21	1.50	approx.			0.0097	0.0094	0.0090	
BC18		98	70	10.63	0.41		13.3		0.0072	0.0070	0.0067	
BC19		133	106	11.32	1.61		16.0		0.0097	0.0094	0.0090	
BC20		194	100	7.64	0.34		13.3		0.0059	0.0057	0.0054	

N	0	P	Q	R	S	T	U	V	W	X	Y	2
SPR	S/N(MF)	@ CReff		S/N(RR)	@ CReff		S/N(MF)	@ CRmin		S/N(RR)	@ CRmin	
Cavern	f=1.0	f-1.43	f=2.0	f=1.0	f=1.43	f-2.0	f=1.0	f-l.43	f=2.0	f=1.0	f-1.43	f=2.0
Label	(dB)	(dB)	(dB)	(dB)	(dB)	(dB)	(dB)	(dB)	(dB)	(dB)	(dB)	(dB)
Bryan Mound Site:												
BM1	44	10	-31	9	-25	-66	94	80	62	66	54	36
BM2	39	4	-39	3	-33	-76	49	18	-20	13	-16	-55
BM4	15	-30	-84	-22	-67	-122	29	-10	-58	-8	-44	-93
BM5	-62	-136	-226	-99	-173	-264	52	21	-16	22	-7	-45
BM101	54	25	-11	25	-4	-40	70	46	17	42	21	-9
BM102	51	20	-18	21	-10	-47	67	42	12	39	16	-15
BM103	50	19	-19	21	-10	-48	66	42	11	38	16	-15
BM104	49	17	-22	19	-13	-51	65	40	9	37	14	-18
BM105	53	23	-14	24	-7	-43	68	44	15	40	19	-12
BM106	46	13	-27	16	-17	-57	63	36	4	34	10	-23
BM107	48	16	-23	18	-14	-53	65	39	8	36	13	-19
BM108	47	15	-25	17	-15	-54	64	38	7	35	12	-20
BM109	50	19	-19	21	-10	-48	66	42	11	36	16	-15
BM110	50	19	-19	20	-11	-49	66	41	11	38	35	-16
BM111	52	21	-16	23	-8	-45	68	43	14	40	18	-13
BM112	54	24	-13	24	-5	-42	69	45	16	41	20	-10
BM113	99	87	72	72	59	44	105	96	83	79	72	59
BM114	96	83	66	68	55	38	103	92	79	76	68	54
BM115	91	76	57	62	47	28	99	87	72	71	61	46
BM116	92	78	59	64	49	31	100	88	74	73	63	48
West Hackberry Site:												
WH6	-116	-211	-327	-155	-250	-366	-66	-142	-235	-104	-178	-272
wH7	56	27	-8	23	-6	-41	73	51	24	42	22	-6
WH8	24	-18	-68	-8	-50	-100	52	21	-16	22	-7	-45
WH9	-44	-112	-194	-80	-148	-230	91	76	57	67	54	35
WH11	21	-21	-73	-11	-54	-105	44	10	-31	13	-19	-60
WH101	89	73	53	59	43	23	97	84	69	69	58	42
WH102	91	75	57	61	46	27	99	87	72	71	61	45
WH103	99	86	71	69	56	41	105	95	83	77	69	56
WH104	103	92	79	73	62	49	109	100	89	80	74	63
WH105	109	100	90	79	71	61	113	107	98	85	81	72
WH106	38	3	-41	8	-28	-71	57	28	-6	28	1	-34
WH107	107	98	87	78	68	57	112	104	95	84	79	69
WH108	96	82	66	66	52	36	103	92	79	74	66	52
WH109	52	21	-16	23	-8	-45	68	43	14	40	18	-13
WH110	82	63	40	53	34	11	92	77	58	64	51	32
WE112	50	19	-19	21	-10	-48	66	42	11	38	16	-15
WH113	80	61	37	50	31	7	91	75	56	62	48	29
WH114	50	19	-19	21	-10	-48	66	42	11	38	16	-15
WH115	51	20	-18	21	-10	-47	67	42	12	39	16	-15
WH116	85	67	46	56	38	16	94	80	63	66	54	36
Bayou Choctaw Site:												
BC15	-31	-93	-169	-66	-129	-205	2	-48	-109	-33	-80	-142
BC17	37	1	-44	6	-30	-75	56	27	-9	26	-1	-37
BC18	73	51	24	44	22	-5	85	67	46	57	42	19
BC19	26	-15	-64	-6	-47	-96	47	14	-25	16	-14	-54
BC20	38	2	-41	3	-33	-76	83	65	42	53	37	14

SAND88-3262 Distribution:

U.S. DOE SPR PMO (9)
900 Commerce Road East
New Orleans, LA 70123
Attn: D. R. Spence, PR-62
E. E. Chapple, PR-622 (5)
D. W. Whittington, PR-622
TDCS (2)

U.S. Department of Energy (1)
Strategic Petroleum Reserve
1000 Independence Avenue SW
Washington, D.C. 20585
Attn: R. Smith

U.S. Department of Energy (1)
Oak Ridge Operations Office
P.O. Box E
Oak Ridge, TN 37831
Attn: B. Manning

DOE SPR Bayou Choctaw Site (2)
P.O. Box 776
Plaquemine, LA 70764
Attn: J. M. Hyde, DOE
Box 1270,
Winnie, TX 77665
A. E. Fruge, DOE

DOE SPR Bryan Mound Site (1)
P.O. Box 2276
Freeport, TX 77541
Attn: C. Bellam, DOE

Boeing Petroleum Services (5)
850 South Clearview Parkway
New Orleans, LA 70123
Attn: J. Siemers (3)
K. Mills
T. Eyermann

Louisiana Geological Survey (1)
University Station; Box G
Baton Rouge, LA 70893
Attn: K. E. Ramsey

Solution Mining Research Institute 812 Muriel Street
Woodstock, IL 60098
Attn: H. Fiedelman

Texas Bureau of Economic Geology (2)
University Station, Box X
Austin, TX 78713
Attn: W. L. Fisher

Walk-Haydel & Associates, Inc.
600 Carondelet St.
New Orleans, LA 70130
Attn: Gary Trochesset

'2174	M. G. Armendariz
2174	D. C. Martin
3141	S. A. Landenberger (5)
3154-l	C. Ward, FOR: DOE/OSTI (8)
3151	W. I. Klein (3)
6000	D. L. Hartley
6200	V. L. Dugan
6230	W. C. Luth
6231	H. C. Hardee
6232	W. R. Wawersik
6232	D. H. Zeuch
6250	R. K. Traeger
6252	J. C. Dunn
6257	J. K. Linn (10)
6257	S. L. Chavez
6257	G. S. Heffelfinger
6257	J. T. Neal
6257	R. L. Parrish
6257	J. L. Todd
6257	S. T. Wallace
6257	S. W. Webb
6258	P. J. Hommert (5)
6258	J. G. Castle (15)
8524	J. R. Wackerly